

Journal Pre-proof

Effects of substituent pattern on the intracellular target of antiproliferative benzo[*b*]thiophenyl chromone derivatives

Yohei Saito, Yukako Taniguchi, Sachika Hirazawa, Yuta Miura, Hiroyuki Tsurimoto, Tomoki Nakayoshi, Akifumi Oda, Ernest Hamel, Katsumi Yamashita, Masuo Goto, Kyoko Nakagawa-Goto

PII: S0223-5234(21)00427-X

DOI: <https://doi.org/10.1016/j.ejmech.2021.113578>

Reference: EJMECH 113578

To appear in: *European Journal of Medicinal Chemistry*

Received Date: 11 February 2021

Revised Date: 9 May 2021

Accepted Date: 19 May 2021

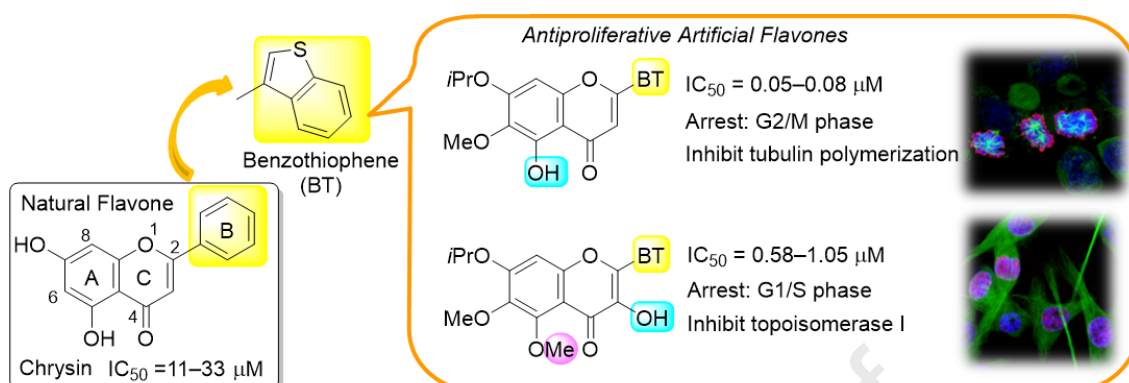
Please cite this article as: Y. Saito, Y. Taniguchi, S. Hirazawa, Y. Miura, H. Tsurimoto, T. Nakayoshi, A. Oda, E. Hamel, K. Yamashita, M. Goto, K. Nakagawa-Goto, Effects of substituent pattern on the intracellular target of antiproliferative benzo[*b*]thiophenyl chromone derivatives, *European Journal of Medicinal Chemistry*, <https://doi.org/10.1016/j.ejmech.2021.113578>.

This is a PDF file of an article that has undergone enhancements after acceptance, such as the addition of a cover page and metadata, and formatting for readability, but it is not yet the definitive version of record. This version will undergo additional copyediting, typesetting and review before it is published in its final form, but we are providing this version to give early visibility of the article. Please note that, during the production process, errors may be discovered which could affect the content, and all legal disclaimers that apply to the journal pertain.

© 2021 Published by Elsevier Masson SAS.



Graphical Abstract



Effects of substituent pattern on the intracellular target of antiproliferative benzo[*b*]thiophenyl chromone derivatives

Yohei Saito,^a Yukako Taniguchi,^a Sachika Hirazawa,^a Yuta Miura,^a Hiroyuki Tsurimoto,^a
Tomoki Nakayoshi,^{b,1} Akifumi Oda,^b Ernest Hamel,^c Katsumi Yamashita,^a Masuo Goto,^{d,*}
Kyoko Nakagawa-Goto^{a,d,*}

^a *School of Pharmaceutical Sciences, College of Medical, Pharmaceutical and Health Sciences, Kanazawa University, Kanazawa, 920-1192, Japan*

^b *Graduate School of Pharmacy, Meijo University, Tempaku-ku, Nagoya, 468-8503, Japan*

^c *Molecular Pharmacology Branch, Developmental Therapeutics Program, Division of Cancer Treatment and Diagnosis, Frederick National Laboratory for Cancer Research, National Cancer Institute, Frederick, Maryland, 21702, United States*

^d *Chemical Biology and Medicinal Chemistry, UNC Eshelman School of Pharmacy, University of North Carolina, Chapel Hill, North Carolina 27599-7568, United States*

Corresponding Authors

* (K.N.G.) Phone: +81-76-264-6305, E-mail: kngoto@p.kanazawa-u.ac.jp

(M.G.) Phone: +1-919-843-6325, E-mail: goto@med.unc.edu

¹(T.N) Current address: Graduate School of Information Sciences, Hiroshima City University, 3-4-1 Ozukahigasi, Asaminami-ku, Hiroshima, Hiroshima 731-3194, Japan

ABSTRACT

A new biological scaffold was produced by replacing the 6π -electron phenyl ring-B of a natural flavone skeleton with a 10π -electron benzothiophene (BT). Since aromatic rings are important for ligand protein interactions, this expansion of the π -electron system of ring-B might change the bioactivity profile. One of the resulting novel natural product-inspired compounds, 2-(benzo[*b*]thiophen-3-yl)-5-hydroxy-7-isopropoxy-6-methoxyflavone (**6**), effectively arrested the cell cycle at the G2/M phase and displayed significant antiproliferative effects with IC_{50} values of 0.05–0.08 μ M against multiple human tumor cell lines, including a multidrug resistant line. A structure-activity relationship study revealed that a 10π -electron system with high aromaticity, juxtaposed 4-oxo and 5-hydroxy groups, and 7-alkoxy groups were important for potent antimitotic activity. Interestingly, two BT-flavonols (3-hydroxyflavone), **16** and **20**, with 3-hydroxy and 5-alkoxy groups, induced distinct biological profiles affecting the cell cycle at the G1/S phase by inhibition of DNA replication through an interaction with topoisomerase I.

Keywords: Benzothiophene, Flavone, Flavonol, Antiproliferative activity, Tubulin, Topoisomerase I

1. Introduction

Enzymes are required for the biosynthesis of all secondary metabolites (natural products) produced by living organisms. With this innate affinity for enzymes, natural products might unexpectedly bind to a protein/enzyme in a different species to produce unpredicted bioactivity. Thus, we can exploit this innate affinity of natural products to discover and develop chemical agents acting at desired protein targets.

Flavonoids are distributed abundantly in plants, including edible fruits and vegetables, as secondary metabolites. They interact with various cellular targets involved in important signal pathways in our bodies and generally act beneficially for human health with relatively low toxicity [1]. Only a few cytotoxic flavonoids have been reported; examples are the highly methoxylated natural flavones centaureidin [2] and 5,3'-dihydroxy-3,6,7,8,4'-pentamethoxyflavone (DH-PMF) [3], which displayed remarkable cytotoxicity ($IC_{50} < 0.5 \mu M$) against human tumor cell lines [4]. These flavones inhibit the assembly of tubulin by binding to the colchicine site (CS).

The basic flavone skeleton has 15 carbons arranged in a C6-C3-C6 unit: two phenyl rings (ring-A and ring-B) connected through a heterocyclic ring (ring-C) containing three carbons and an oxygen atom. They are classified based on the oxidation stage of ring-C, e.g., flavone, flavonol (3-hydroxyflavone), flavanone (2,3-dihydroflavone), etc., and the attachment of ring-B (flavone vs. isoflavone). Except for isoflavones, a common flavone structure (2-phenyl-4-chromone) has fused benzene and pyran-4-one rings (ring-A and -C, respectively) with a phenyl group (ring-B) attached at C-2 (Figure 1).

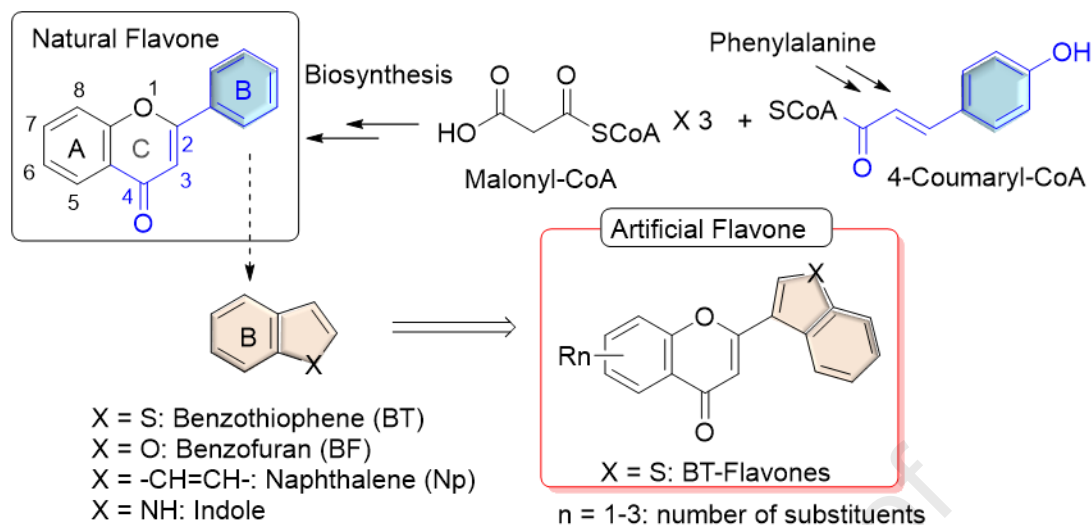


Figure 1. Natural Flavone Skeleton and Proposed Artificial Flavone

Because the basic three-ring system is biosynthesized from 4-coumaroyl-CoA derived from phenylalanine and three malonyl-CoAs, the ring-B in naturally occurring flavones is normally a phenyl group, a 6π -electron aromatic ring. Aromatic ring systems in bioactive compounds often play an important role in binding to target proteins or enzymes [5-7]. They are rigid, hydrophobic, structurally planar, and π electron rich, which can stabilize ligand-protein binding through π stacking, cation- π , and OH/ π interactions [8]. Bicyclic aromatic units, such as benzothiophene (BT), benzofuran (BF), and naphthalene (Np), are 10π -electron rather than 6π -electron systems; the electron distribution expands over an additional 4π -orbitals. The higher aromaticity might impact biological profiles, including absorption, distribution, metabolism, and excretion (ADME) properties [9-12]. Thus, we postulated that a novel biological backbone (Figure 1) could result from connecting a chromone to a bicyclic aromatic system rather than the phenyl ring-B present in the natural flavone skeleton.

Among 10π aromatic systems, the BT skeleton is rarely found in secondary metabolites [13], although it is often found in various clinical drugs [14]. The sulfur atom in BT contributes to

higher aromaticity through its 3d orbital, and its electronegativity is close to that of carbon. Other 10π systems, including BF, Np, and indole ($X = \text{NH}$), are biosynthesized through acetyl CoA as well as shikimic acid and are abundant in natural products.

Previously, we found a dramatic change between the bioactivity profiles of triethyldesmosdumotin B (TEDB) and TEDB-BT, which differ structurally only in ring-B: phenyl in TEDB versus BT in TEDB-BT (Figure 2) [15-17]. TEDB is a derivative of desmosdumotin B (DesB), an atypical flavonoid with a non-aromatic ring-A. It effectively inhibited the growth of a multi-drug resistant (MDR) tumor cell line, while it was non-toxic against the tested chemosensitive tumor cell lines. This unique biological phenomenon is called collateral sensitivity [18]. However, TEDB-BT displayed potent cell growth inhibition against multiple tumor cell lines and inhibited tubulin polymerization, potentially through the CS [17,19]. In addition, several BT derivatives were recently reported as potent antimetabolic agents [20-27].

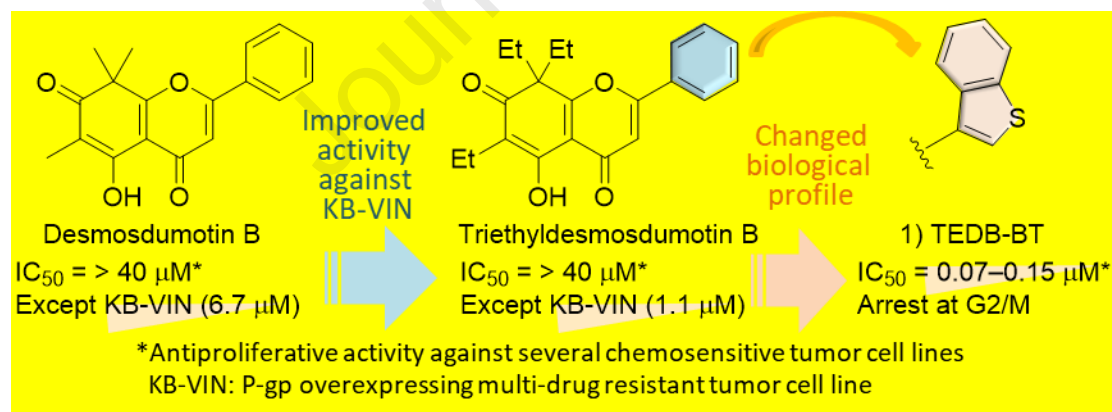


Figure 2. BT Effect on Desmosdumotin B

This notable effectiveness of BT strongly encouraged us to synthesize novel scaffolds, specifically, the hybrids of chromones with bicyclic aromatic rings, including BT. Herein, we

discuss the syntheses, structure-activity relationship of BT-flavones and their mechanism of action.

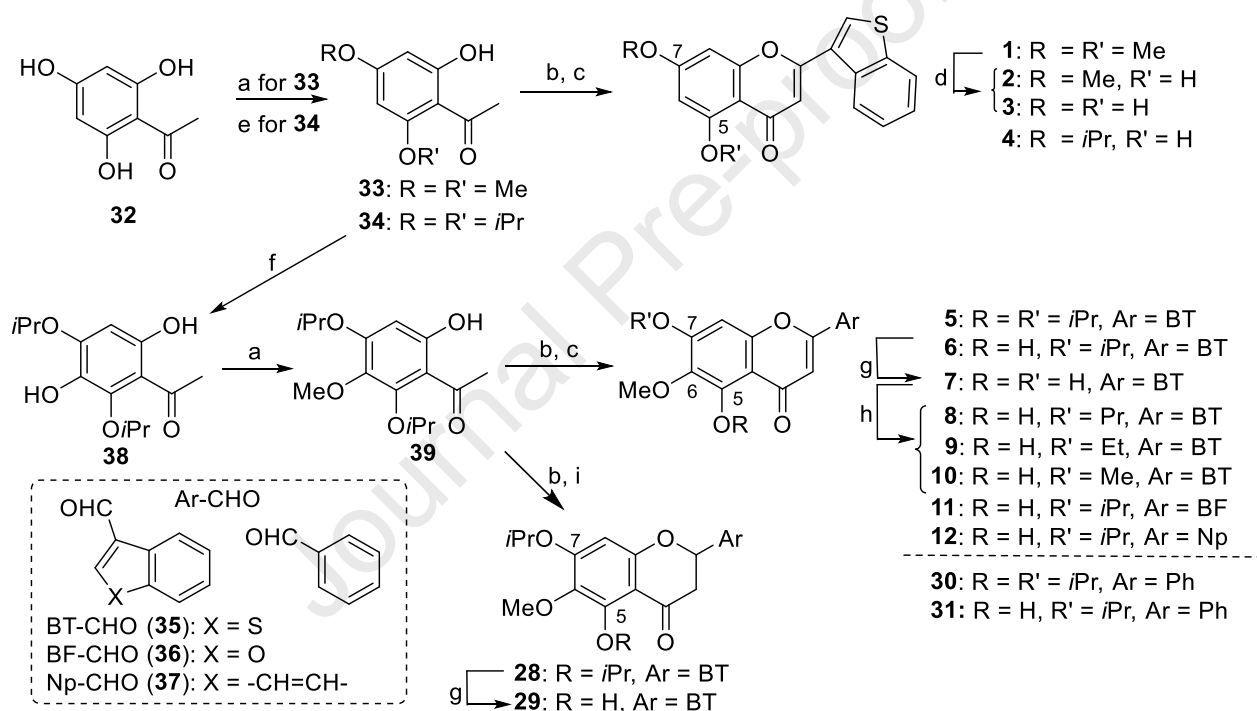
2. Results and discussion

2.1 Chemistry

All flavones were prepared by traditional flavone synthetic methods through Claisen-Schmidt condensation for **1–13**, **30** and **31** (Schemes 1 and 2) or Baker-Venkataraman rearrangement for 3-substituted derivatives **14–27** (Scheme 3). Trihydroxyacetophenone **32** was the best candidate as a starting material for di-substituted and tri-substituted BT-flavones (Scheme 1). The standard methylation and isopropylation of the two phenolic hydroxy groups on **32** produced dimethoxy **33** and di-isopropoxy **34**, respectively. The Claisen-Schmidt condensation of **33** and **34** with BT-3-carbaldehyde (**35**), followed by I₂ catalyzed cyclization, yielded the related flavones **1** and **4**, respectively. With the latter compound, the isopropyl group at C-5 was lost during the cyclization step to leave a hydroxy moiety. The treatment of **1** with BBr₃ produced monomethoxy **2** and dihydroxy **3**. In an Elbs persulfate oxidation, a hydroxy group was added to **34** to give **38**, which was then methylated to yield **39** [28]. A Claisen-Schmidt condensation of **39** with BT-3-carboxaldehyde (**35**) followed by cyclization produced tri-substituted flavones **5** and **6**. Again, in the latter compound, the isopropyl group on the 5-OH of the starting material was spontaneously removed during the cyclization. The remaining isopropyl group in **6** was eliminated by using AlCl₃, and the 5-OH in the resulting 5,7-dihydroxy BT-flavone **7** was selectively alkylated to produce 5-propoxy **8**, 5-ethoxy **9**, and 5-methoxy **10**. Alternatively, the treatment of **39** with benzofuran-3-carbaldehyde (**36**) [29] or 1-naphthaldehyde (**37**) produced the related flavones **11** and **12**, respectively. For comparison purposes, typical flavones **30** and **31**

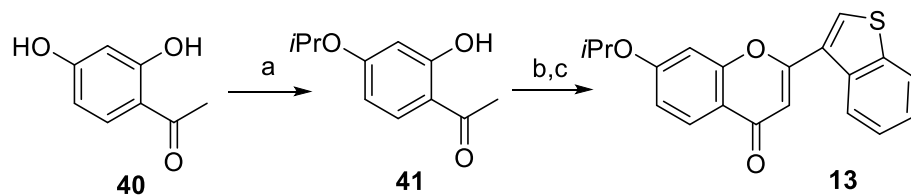
with a phenyl ring-B were also synthesized from **39** and benzaldehyde. Claisen-Schmidt condensation of **39** with **35** followed by acidic treatment produced 2,3-dihydroflavone **28** as a racemate. The removal of the isopropyl group on the 5-OH generated **29**, which is equivalent to **6**, except for the oxidation state of the C2-C3 bond (single bond in **29**, double bond in **6**).

Mono-substituted flavone **13** was prepared from resacetophenone (**40**) through the selective isopropylation of a phenolic hydroxy group, followed by Claisen-Schmidt condensation with **35** and cyclization with catalytic I₂ in dimethyl sulfoxide (DMSO) (Scheme 2).



Scheme 1. Preparations of Di- and Tri-substituted BT-Flavones 1–12 and 28–31

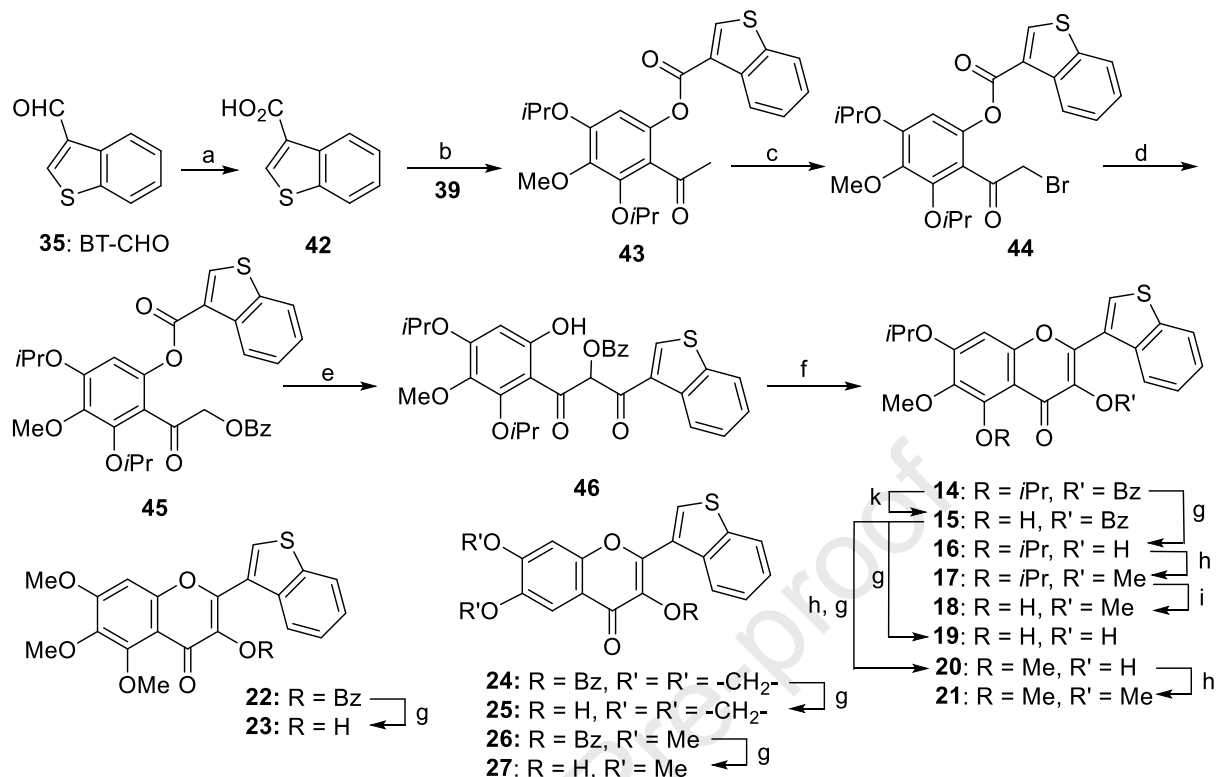
Reagents and conditions: a) Me₂SO₄, K₂CO₃, DMF, 80 °C; b) 50% KOH aq., EtOH, rt for BT-CHO (**35**), Np-CHO (**37**), or PhCHO, Ba(OH)₂, DMF, 90 °C for BF-CHO (**36**); c) I₂ (cat.), DMSO, 180 °C; d) BBr₃, CH₂Cl₂, 0 to 45 °C; e) *i*PrBr, K₂CO₃, DMF, 80 °C, 3.5 h; f) K₂S₂O₈, NaOH, Py, rt; g) AlCl₃, CH₂Cl₂, 0 °C to rt; h) RI (R = Et for **9**, R = Pr for **8**) or Me₂SO₄ for R = Me, K₂CO₃, acetone, reflux; i) NaOAc, EtOH, H₂O, 80 °C.



Scheme 2. Preparation of Mono-substituted BT-Flavone 13

Reagents and conditions: a) *i*PrBr, K₂CO₃, DMF, 80 °C, 3.5 h; b) BT-CHO (**35**), 50% KOH aq., EtOH, rt; c) I₂ (cat.), DMSO, 180 °C.

3-Substituted BT-flavones were prepared by Fougere's method [30] through a Baker-Venkataraman rearrangement (Scheme 3). The hydroxy group on **39** was condensed with the carboxylic acid of **42**, derived from **35**, to yield ester **43**. Then, the α position on the acetyl group was selectively brominated by using phenyltrimethylammonium tribromide to produce **44**, which was treated with potassium benzoate to generate **45**. A Baker-Venkataraman rearrangement of **45** was performed with sodium hydride in THF, and the resulting 1,3-diketone **46** was cyclized under acidic conditions to form 3-benzoylated BT-flavone **14**, which was treated with TiCl₄ to obtain its de-isopropyl analog **15**. Basic hydrolysis of **14** with NaOH produced the related 3-hydroxy BT-flavone **16**. Further treatment of **16** with Me₂SO₄ produced **17**, which was reacted with aluminum trichloride for selective removal of the isopropyl group to give **18**. Hydrolysis of **15** produced 3,5-dihydroxy BT-flavonol **19**, a 3-hydroxy analog of **6**. Methylation of the 5-OH of **15**, followed by hydrolysis of the benzoate, generated **20**. Subsequently, the 3-OH of **20** was methylated to obtain 3,5,6-trimethoxy **21**. The same sequence of reactions using 6-hydroxy-2,3,4-trimethoxyacetophenone [31], 2-hydroxy-4,5-methylenedioxyacetophenone [32], or 2-hydroxy-4,5-dimethoxyacetophenone [33] provided benzoates **22**, **24**, and **26**, respectively, which were then hydrolyzed to produce **23**, **25**, and **27**, respectively.



Scheme 3. Preparations of 3-Substituted BT-Flavones 14–27

Reagents and conditions: a) Jones Reagent, acetone; b) EDCI, DMAP, CH₂Cl₂, rt; c) PhMe₃N⁺Br₃⁻, THF, rt; d) PhCOOK, CH₃CN, reflux; e) NaH, THF, 65 °C; f) 2.5% H₂SO₄/AcOH, 60 °C; g) 5% NaOH, EtOH, 60 °C; h) Me₂SO₄, K₂CO₃, DMF, 80 °C; i) AlCl₃, CH₂Cl₂, 0 °C to rt; k) TiCl₄, CH₂Cl₂, 0 °C to rt.

2.2. Biological Evaluation

2.2.1. Antiproliferative effects and SAR analysis

The newly synthesized flavones and flavonols were evaluated for antiproliferative activity against five human tumor cell lines: A549 (lung carcinoma), two breast cancer cell lines (MDA-MD-231 and MCF-7), KB (cervical cancer cell line derived from HeLa cells), and the KB-subline KB-VIN showing the MDR phenotype with overexpression of the drug transporter P-glycoprotein (P-gp) (Tables 1 and 2). Paclitaxel, a cytotoxic, antitubulin P-gp substrate, was used as an experimental control. The antiproliferative effects of the compounds were measured with a sulforhodamine B (SRB) assay, and IC₅₀ values were calculated from at least three independent

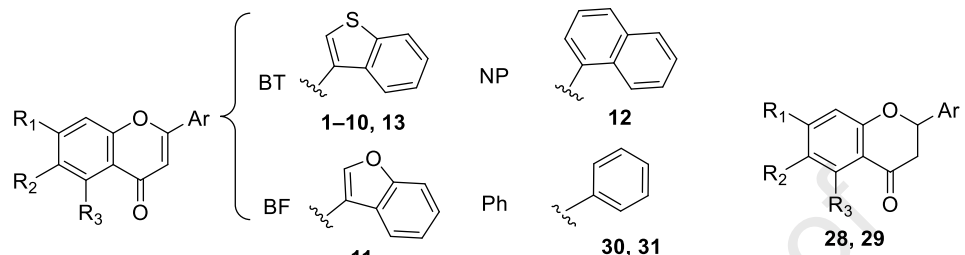
experiments, each performed in duplicate. For comparison, IC₅₀ values obtained with a typical flavone, chrysin (5,7-dihydroxyflavone), were also obtained.

Among all compounds, five (three 2-(benzo[*b*]thiophen-3-yl)-5-hydroxy-6-methoxy-7-alkoxyflavones [R₁ = alkoxy, R₂ = OMe, R₃ = OH, Ar = BT (**6**, **8**, and **9**); the naphthyl derivative **12**; and the flavanone **29**) showed potent antiproliferative activity (IC₅₀ 0.05–0.12 μM) against all tested tumor cell lines, including the MDR cell line, KB-VIN (highlighted in Table 1). These compounds were dramatically more potent as compared to the related flavone **31** with a phenyl ring-B (IC₅₀ = 8.95–29.1 μM). These results demonstrated a key effect with BT or Np as ring-B.

In contrast, compound **3** (BT-chrysin) did not show improved potency as compared to natural chrysin. However, while most natural flavones exhibit only moderate to weak cytotoxicity, a few highly functionalized flavones were exceptions. For instance, 5,3'-dihydroxy-3,6,7,8,4'-pentamethoxyflavone, first isolated in 1986 from *Gutierrezia microcephala* [34], showed potent antimitotic antiproliferative activity with IC₅₀ values of 0.08 and 1.49 μM against KB and A549 cells, respectively [35]. Lewin's group vigorously pursued further research on cytotoxic flavonoids and concluded that a 5-hydroxy-6,7,8-trimethoxy arrangement on ring-A and 3-hydroxy/3-amino-4-methoxy groups on ring-B were the most favorable substitution patterns for increased potency [36]. However, our study suggests the importance of the aromaticity of ring-B, with a 10π electron system significantly influencing antiproliferative activity. The order of potency in our assays was **6** ≥ **12** > **11**, which correlated with the order of ring-B aromaticity, BT ≥ Np > BF. Because the electronegativities of sulfur (BT), carbon (Np), and oxygen (BF) atoms are 2.5, 2.5 and 3.5, respectively, the lone pair delocalization is less effective on the oxygen than on the sulfur and carbon atoms, which reduces the aromaticity of BF. In addition, the 3d orbital

of the sulfur atom efficiently contributes to resonance. As noted above, flavone **31** with the natural 6π -electron ring-B (phenyl) was substantially less potent as compared to the compounds with a 10π -electron ring-B.

Table 1. Antiproliferative Activities of Synthesized Flavones 1–13 and 28–31.



Compounds	Human cancer cell lines ^a /IC ₅₀ (μM) ^b								
	R ₁	R ₂	R ₃	Ar	A549	MDA-MB-231	MCF-7	KB	KB-VIN
1	OMe		OMe		10.8	>40	>40	36.8	13.3
2	OMe	H			36.3	>40	>40	>40	>40
3	OH		OH		20.5	29.9	24.7	24.9	19.3
4					8.41	8.34	8.53	8.74	5.88
5	OiPr		OiPr		7.23	11.8	7.48	5.84	6.06
6	OiPr			BT	0.05	0.08	0.08	0.07	0.06
7	OH	OMe			23.3	37.3	9.84	20.6	18.5
8	OPr		OH		0.07	0.08	0.07	0.06	0.05
9	OEt				0.07	0.07	0.07	0.06	0.05
10	OMe				0.44	0.50	0.70	0.57	0.37
13		H	H		6.83	18.8	6.77	5.34	4.31
11				BF	0.19	0.25	0.52	0.31	0.09
12	OiPr		OH	Np	0.08	0.12	0.08	0.10	0.09
30		OMe	OiPr		31.1	40.2	32.2	35.3	33.0
31			OH	Ph	10.1	29.1	18.0	22.4	8.95
Ch ^c	OH	H	OH		28.0	33.0	26.9	29.6	11.5
28	OiPr	OMe	OiPr	BT	5.40	16.8	8.23	4.84	1.91
29	OiPr	OMe	OH	BT	0.06	0.09	0.10	0.06	0.06
Paclitaxel					0.0057	0.00917	0.0633	0.00579	2.105

^a A549 (lung carcinoma), MDA-MB-231 (triple-negative breast cancer), MCF-7 (estrogen receptor-positive & HER2-negative breast cancer), KB (cervical cancer cell line derived from HeLa cells). ^b Antiproliferative activity as IC₅₀ values for each cell line, the concentration of compound that caused 50% reduction relative to untreated cells determined by the SRB assay. Each experiment was performed three times, and standard deviations were within 10% of the means (see Supplemental Table S1). ^c Chrysin

Among the flavones with no substituent at C-3 (Table 1), the combination of 5-hydroxy (R₃ = OH), 6-methoxy (R₂ = OCH₃) and 7-alkoxy (R₁ = O-alkyl) substitution in ring-A was crucial for

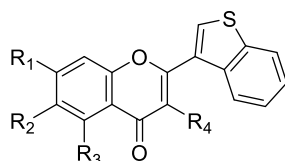
potent antiproliferative activity. The size of the 7-alkoxy group also influenced activity. A comparison of the results obtained with **6** and **8–10** showed that compound **10** with a 7-methoxy group was clearly less potent (IC_{50} 0.37–0.70 μ M) than **6** (isopropoxy), **8** (propoxy), and **9** (ethoxy) with larger alkoxy groups (IC_{50} 0.05–0.08 μ M). In addition, compound **7**, which differs from **6** and **8–10** only by a 7-hydroxy instead of a 7-alkoxy group, dramatically lost activity ($IC_{50} > 10$ μ M). The 5-hydroxy moiety ($R_3 = OH$), which could form a hydrogen bond with the ketone at C-4, was another key for better activity. Compound **5** with a 5-isopropoxy group clearly showed decreased cell growth inhibition as compared to **6** with a 5-hydroxy group. Flavanone **29** and flavone **6** exhibited significant potency with similar IC_{50} values. Since the two compounds have identical structures except for the saturated C2-C3 bond in ring-C of the former compound, a double bond between C-2 and C-3 is not crucial. The comparable results for flavanone **28** and the analogous flavone **5** were consistent with this conclusion.

Notably, most derivatives displayed similar antiproliferative effects against KB-VIN, a P-gp-overexpressing MDR tumor cell line, and the chemosensitive tumor cell lines. This finding indicates that these compounds are not P-gp substrates and could be effective against MDR tumors. Moreover, compounds **1**, **11**, and **31** exhibited collateral sensitivity [18], showing two- to three-fold greater antiproliferative activity against KB-VIN than the parental non-MDR tumor cell line, KB.

Among the synthesized flavonols (**14–20**), compounds **15** and **18–20** exhibited the highest activity (IC_{50} 0.24–1.05 μ M) (Table 2), although they were generally tenfold less potent than flavones **6**, **8**, and **9** and compounds **12** and **29**. At C-3 (R_4), flavonols **19** and **20** have a free OH, and flavonols **15** and **18** have benzoate and methoxy groups, respectively, indicating some tolerance in the substitution at this position. At C-7 (R_1) and C-6 (R_2), all four active flavonols

have isopropoxy and methoxy substituents, respectively, while at C-5 (R_3), three compounds (**15**, **18**, **19**) have a hydroxy, and flavonol **20** has a methoxy group. Compounds **24–27**, with no substituent on C-5, were clearly less active, suggesting the importance of a hydroxy/alkoxy group at C-5. Comparison of the data for **20** and **23** indicated the same SAR effect found with flavones **6** and **10**. The compound with the larger 7-isopropoxy group (**20**) was more potent than the compound with the smaller 7-methoxy moiety (**23**).

Table 2. Antiproliferative Activities of Synthesized Flavonols 14–27.^a



14–27

Compounds				Cell lines/IC ₅₀ (μM)				
R ₁	R ₂	R ₃	R ₄	A549	MDA-MB-231	MCF-7	KB	KB-VIN
		O <i>i</i> Pr	OBz	3.87	6.62	6.42	5.64	6.38
		OH	OBz	0.64	0.75	0.81	0.56	0.55
		O <i>i</i> Pr	OH	5.08	6.62	6.19	5.96	6.02
			OMe	17.8	27.4	21.6	19.0	14.7
O <i>i</i> Pr			OH	0.36	0.71	0.45	0.25	0.24
	OMe		OH	0.93	2.58	7.43	0.87	0.64
			OH	0.58	1.00	1.05	0.65	0.68
		OMe	OMe	5.31	8.97	7.72	5.37	4.83
			OBz	5.23	7.78	6.46	5.29	4.59
	OMe		OH	6.04	11.5	7.92	8.06	6.97
	-OCH ₂ O-		OBz	4.47	7.31	6.70	5.32	4.70
		H	OH	8.10	10.1	>40	>40	>40
	OMe		OBz	5.20	8.81	8.04	6.25	6.52
	OMe		OH	6.76	18.3	23.1	18.6	13.1
Paclitaxel				0.0057	0.00917	0.00633	0.00579	2.105

^a Each experiment was performed three times, and standard deviations were within 10% of the means (see Supplemental Table S2).

It is noteworthy that compound **6** showed 45-fold lower antiproliferative activity against human umbilical vein endothelial cells (HUVECs), with an IC_{50} value of 2.26 μ M, indicating that **6** selectively inhibited the growth of tumor cells. Next, the biological effects and targets of the new synthetic flavones were examined to clarify the different SAR observations.

2.2.2. Identification of cell cycle phases affected by compound modifications

To determine the cellular target of the active compounds, the initial mechanism of action (MOA) studies were performed using flavone **6**. Because TEDB-BT, the BT modified atypical flavonoid, induces cell cycle arrest at G2/M by inhibiting tubulin polymerization [17,19], the effects of **6** on cell cycle progression and tubulin polymerization were analyzed by flow cytometry and immunocytochemistry (Figure 3). Compound **6** induced cell cycle arrest at G2/M in a dose-dependent manner. The immunostaining of **6**-treated cells with antibodies to α -tubulin and Ser10-phosphorylated histone H3 (p-H3), a mitotic marker of condensed chromosomes, as well as with 4',6-diamidino-2-phenylindole (DAPI) for DNA, clearly demonstrated that depolymerization of microtubules and abnormal centrosomal amplification with immature spindles had occurred in p-H3-positive cells. These results confirmed that compound **6** induced cell cycle arrest at prometaphase by targeting tubulin. The phenotype of cells treated with an equitoxic concentration of combretastatin A-4 (CA-4), a CS tubulin polymerization inhibitor, differed from that of **6**-treated cells in that no p-H3-positive chromosome condensation occurred, suggesting that **6** and CA-4 may target tubulin by slightly different mechanisms.

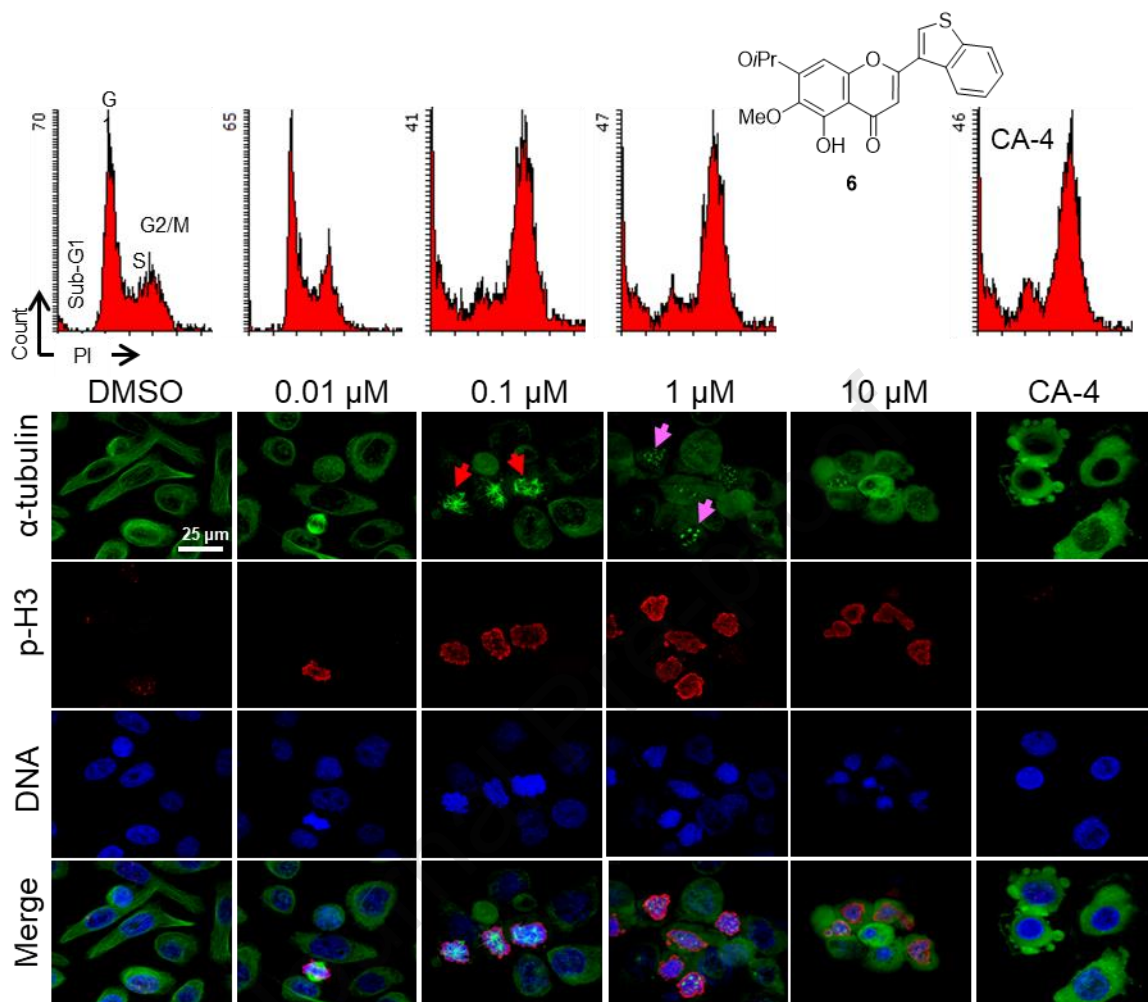


Figure 3. Dose-dependent Effects of 6 on Cell Cycle Progression, Microtubules, and Spindle Formation. PC-3 cells were treated with 6 for 24 h at the indicated compound concentrations. DMSO was used as a vehicle control. Cell cycle distributions of treated cells were analyzed by flow cytometry after staining with PI. A CS tubulin polymerization inhibitor combretastatin A-4 (CA-4) was used at 200 nM as a control for accumulation of G2/M phase cells. Treated cells were triple-stained with antibodies to α -tubulin (green), Ser10-phosphorylated histone H3 (p-H3, red), a marker of mitotic chromosome condensation, and DAPI (blue) for DNA. Stained cells were observed with a confocal fluorescence microscope. The represented merged image was a projection of 16-24 optical sections. Multipolar immature spindles (red arrows), abnormal amplification of spindle poles without spindle elongation (pink arrows). Bar, 0.025 mm.

To ascertain whether compounds with various ring-B types affected cell cycle and mitotic inhibition differently, cells treated with natural chrysin and four additional synthetic flavones (**8**, **11**, **12**, **31**) were also analyzed by flow cytometry and immunocytochemistry. The natural compound and all four synthetic analogues showed the same effect as **6** on mitotic progression (Figure 4), although they exhibited different IC_{50} values in the antiproliferative assays. Four compounds, **31**, **12**, **11**, and **6**, have the same substituted chromone connected to a different ring-B, Ph, Np, BF, and BT, respectively. From an overall evaluation of bioactivity based on IC_{50} and induction of cell cycle arrest at G2/M, the effects of ring-B were conjectured to follow the order, Ph (**31**) \ll BF (**11**) $<$ Np (**12**) \leq BT (**6**), which correlated well with the order of ring aromaticity.

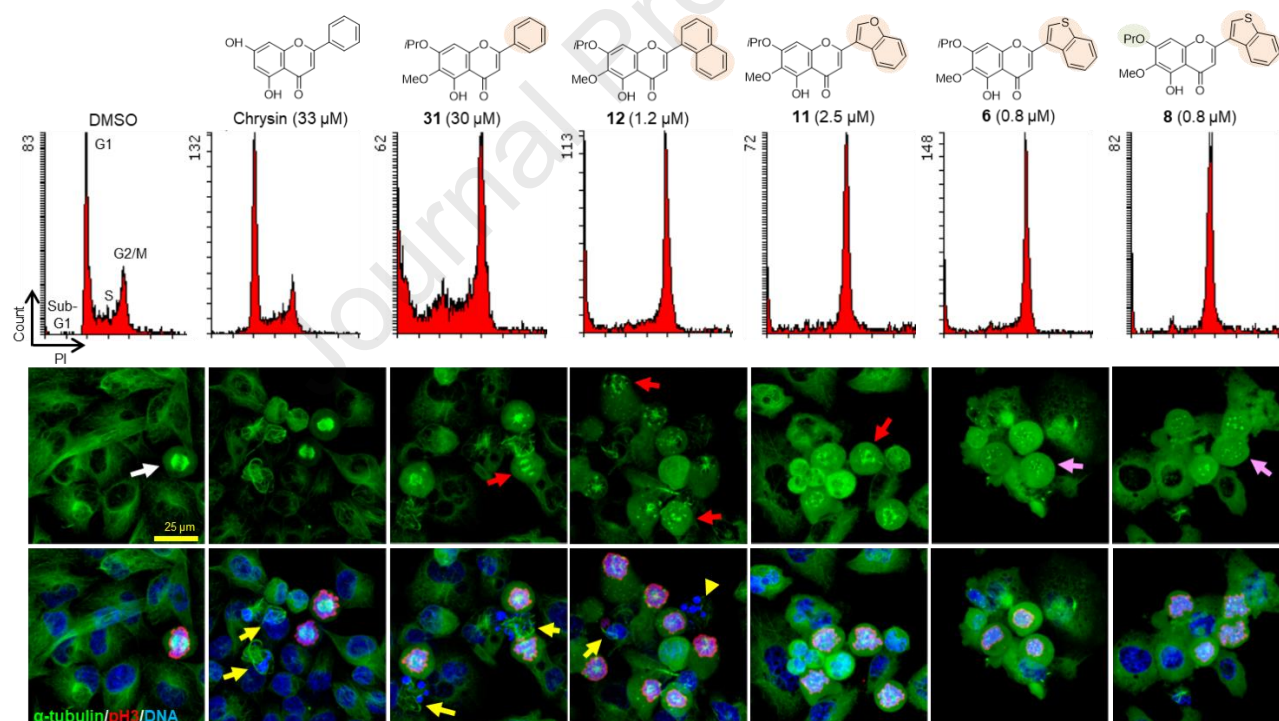


Figure 4. Effect of Ring-B on Induction of G2/M Arrest.

MDA-MB-231 cells were treated with compound for 24 h at the indicated concentrations. DMSO was used as a vehicle control. Treated cells were subjected to analysis of the effects on cell cycle progression by flow cytometry and immunocytochemistry. Cell cycle distributions of treated cells were analyzed by flow cytometry after staining with PI. Treated cells were triple-stained with antibodies to α -tubulin (green), Ser10-phosphorylated histone H3 (p-H3, red), a marker of mitotic chromosome condensation, and DAPI (blue) for DNA. Stained cells were

observed with a confocal fluorescence microscope. The represented merged image was a projection of 18-24 optical sections. Normal bipolar spindles (white arrow), multipolar immature spindles (red arrows), amplification of spindle poles without spindle elongation (pink arrows), cells with nuclear fragmentation with apoptotic microtubules (yellow arrows), fragmented and dispersed chromatin (yellow arrowhead). Bar, 0.025 mm.

The effects of ring-A substituents in **4–6**, **8**, and **9** on mitotic arrest were also analyzed by flow cytometry (Figure 5). A 5-hydroxy group was critical (see **5** vs **6**) and a 6-methoxy group improved the induction of cell cycle arrest at G2/M (see **4** vs **6**).

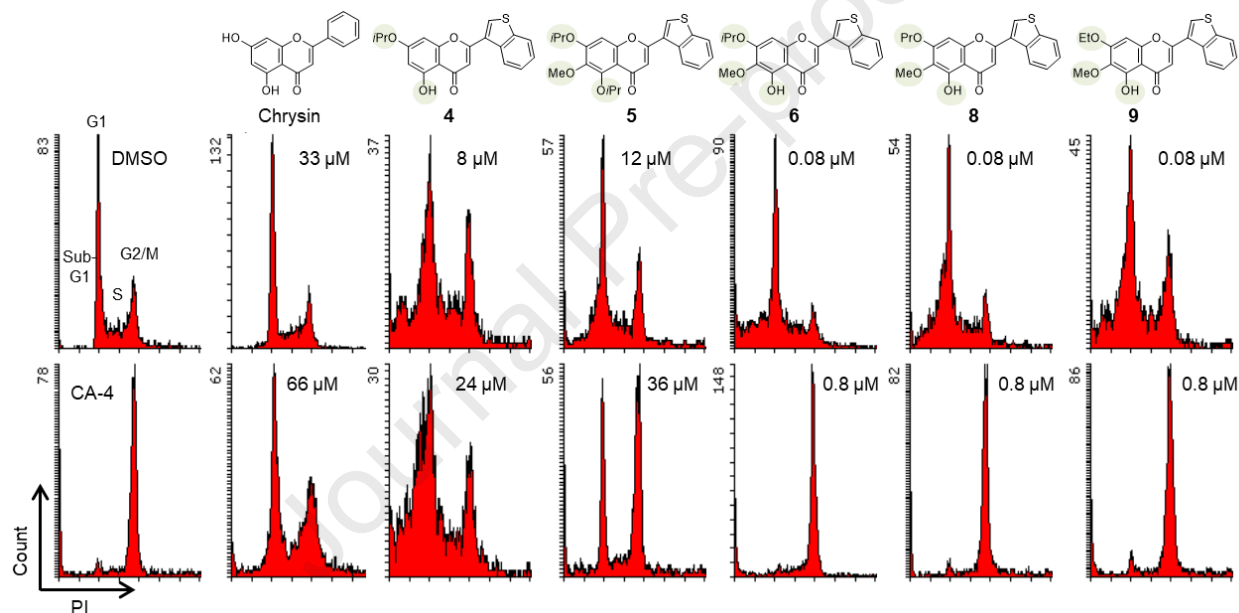


Figure 5. Effect of Ring-A Modification on Induction of G2/M Arrest.

MDA-MB-231 cells were treated with compound for 24 h at the indicated concentrations. DMSO or 200 nM CA-4 ($10\times$ IC_{50}) was used as a vehicle control or tubulin polymerization inhibitor arresting cells at G2/M, respectively. Cell cycle distributions of treated cells were analyzed by flow cytometry after staining with PI.

The MOA studies were also conducted on the four bioactive flavonols **16**, **18**, **19**, and **20**. Flow cytometric analysis of cells treated with flavonols **18** and **19**, which, like **6**, have a 5-OH, displayed accumulation of cells in the G2/M phase after 24 h (Figure 6), similar to that found with CA-4, regardless of their 3-alkoxy or -hydroxy group. In contrast, flavonols **20** and **16**, which, in addition to a 3-OH, possess a 5-alkoxy rather than hydroxy group, showed a different effect on the cell cycle. Both compounds impacted cell cycle progression at the G1/S phase (Figure 7), not the G2/M phase. Thus, a 5-OH is likely crucial for the compound to target tubulin and arrest cells at G2/M. Furthermore, compounds with both 3-hydroxy and 5-alkoxy groups affected the G1/S phase, instead of the G2/M phase. These results suggested that the 3-OH and 5-OH are key factors in determining the target of the flavonols.

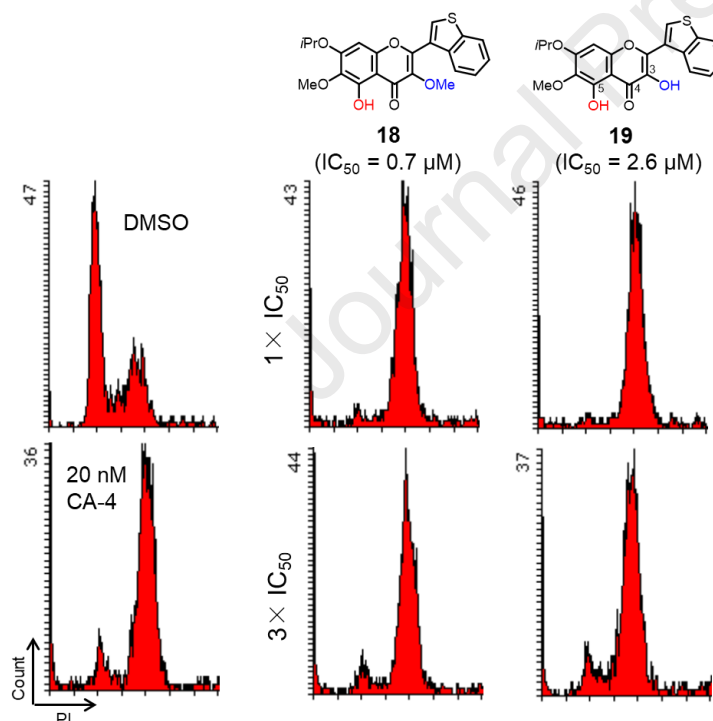


Figure 6. Effects of Flavonols 18 and 19 on Induction of G2/M Arrest.

MDA-MB-231 cells were treated with compound **18** or **19** for 24 h at 1-fold ($1 \times IC_{50}$) or 3-fold ($3 \times IC_{50}$) the IC_{50} values. DMSO or 20 nM CA-4 ($1 \times IC_{50}$) was used as a vehicle control or tubulin polymerization inhibitor arresting cells at G2/M, respectively. Cell cycle distributions of treated cells were analyzed by flow cytometry after staining with PI.

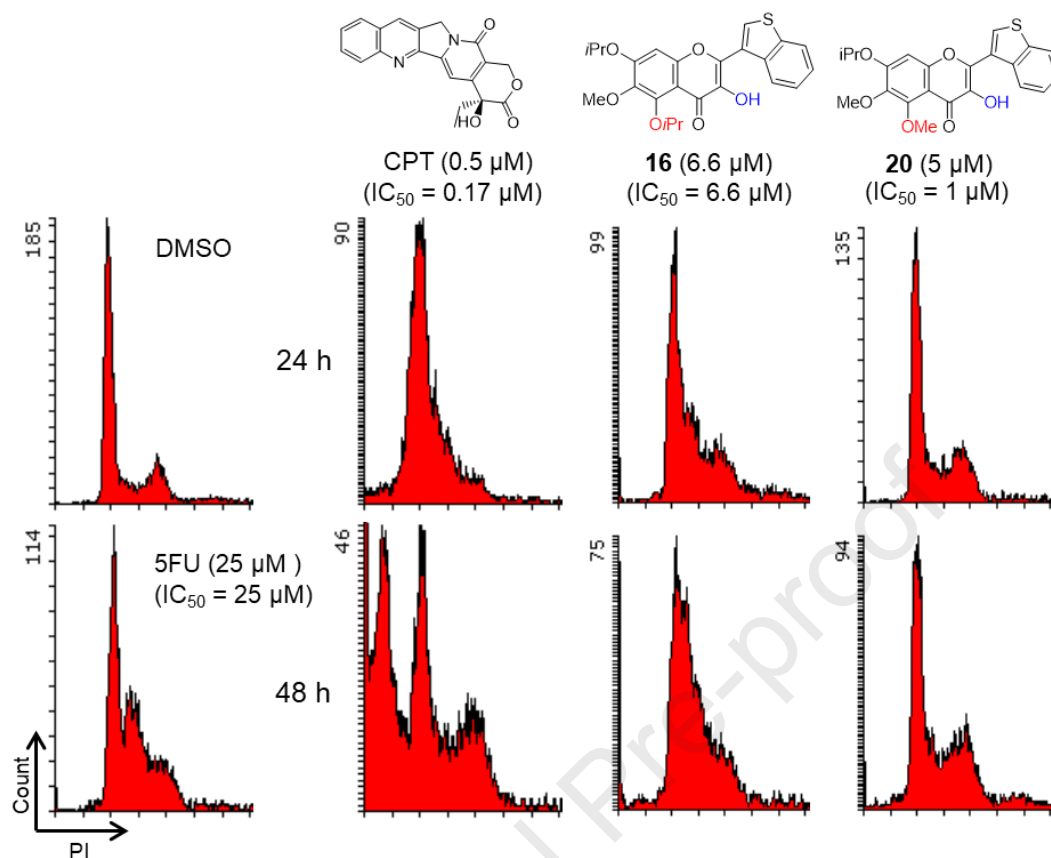


Figure 7. Effects of Flavonols 16 and 20 on Accumulation of Cells in S-phase.

MDA-MB-231 cells were treated with compound **16**, **20**, or reference compound 5-FU or CPT for 24 or 48 h at the indicated concentrations. DMSO was used as a vehicle control. Cell cycle distributions of treated cells were analyzed by flow cytometry after staining with PI.

The S phase in the cell cycle is involved in DNA replication. Camptothecin (CPT) and 5-fluorouracil (5-FU) are well-known agents that damage DNA through different mechanisms of action, which can be distinguished by analyzing the distribution of cells in the cell cycle. Based on the flow cytometric analysis, compound **16** and 5-FU act by a similar mechanism, showing cell accumulation at the S phase, while **16** is 3.8-fold more potent than 5-FU (Figure 7). Meanwhile, the cell cycle distributions with **20** and CPT were similar (Figure 7); thus, the likely molecular target of **20** is topoisomerase (Topo) I, which is the target of CPT. When DNA is damaged, its repair pathway is activated, which leads to the induction of phosphorylated histone

H2AX (γ H2AX). To confirm the DNA damage, the cells treated with flavonols **16**, **18**, **19**, and **20** were stained with antibodies to α -tubulin and γ H2AX as well as DAPI for DNA (Figure 8). Among the four compounds, the 3-hydroxy analogues **16** and **20** clearly induced DNA damage as did the control 5-FU. Considering the immunostaining and flow cytometry results, it is postulated that **16** acts similarly to 5-FU, by impairing DNA replication through depletion of newly synthesized nucleotides [37]. In contrast, compounds **18** and **19** did not show significant induction of γ H2AX positive cells, while they did inhibit tubulin polymerization with abnormal centrosomal amplification; thus, like **6**, these two compounds target tubulin.

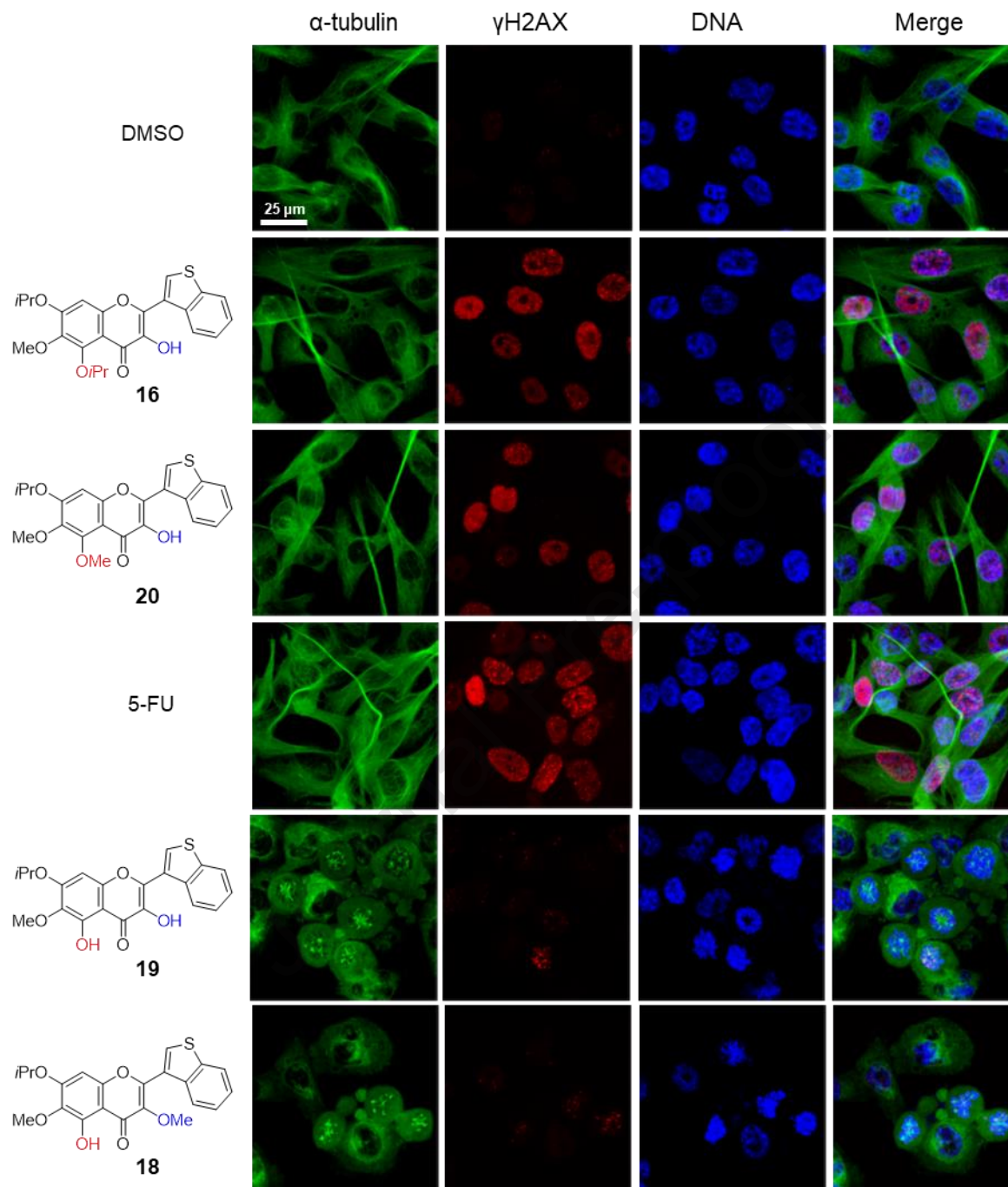


Figure 8. Induction of DNA Damage by Compounds.

MDA-MB-231 cells were treated with compounds **16**, **18**, **19**, or **20** for 24 h at the IC_{50} concentrations. DMSO or 5-FU was used as a vehicle control or positive control, respectively. Treated cells were triple-stained with antibodies to α -tubulin (green), γ -H2AX (red), a marker of DNA double-strand breaks (DSBs), and DAPI (blue) for DNA. Stained cells were observed by confocal fluorescence microscopy. The merged images shown were projections of 16-20 optical sections. Bar, 0.025 mm.

2.3. Molecular MOA

2.3.1. Effect of 3-OH flavones on tubulin polymerization and colchicine binding to tubulin

Antitubulin agents binding to the CS, including CA-4, disrupt cell cycle progression at the G2/M phase. Selected antiproliferative flavones were evaluated in a cell-free system to evaluate a direct inhibitory effect on tubulin assembly (ITA), as measured by turbidimetry, and for inhibition of [³H]colchicine binding to tubulin, *i.e.*, whether compounds could compete with colchicine. The 50% effective concentration for inhibiting tubulin assembly (IC₅₀) and percent inhibition of colchicine binding to tubulin (ICB) of flavones **6**, **8**, and **9**, flavonols **16** and **18–20**, and flavanone **29** were determined (Table 3). Typical turbidimetry experiments are shown in Supplemental Materials, Fig. S76, for compounds **18** (Panel A), **8** (Panel B) and **20** (Panel C). As expected, flavone **6** strongly inhibited tubulin assembly with an IC₅₀-ITA value of 1.3 μM; it also inhibited colchicine binding by 61%. Flavanone **29** showed similar inhibitory effects to those of **6**, indicating that both sp³ and sp² carbons at C2 and C3 were tolerated for inhibition of tubulin. The size of the 7-alkoxy group influenced the inhibition of tubulin assembly as well as apparent binding to the CS. While compound **8** with a 7-propoxy group exhibited an IC₅₀-ITA value of 1.9 μM, it was less effective than **6** with a 7-isopropoxy group at inhibiting colchicine binding to tubulin. 7-Ethoxy derivative **9** did not significantly inhibit tubulin assembly in the cell-free system, while its *in vitro* antiproliferative activities were almost identical to those of **6** and **9**. Like flavone **6**, 5-hydroxy-3-methoxy flavonol **18** mildly inhibited colchicine binding to tubulin, but it showed a potent inhibitory effect on tubulin assembly. As predicted from the results of flow cytometry and immunocytochemical analysis, 5-alkoxy flavonols **16** and **20** did not inhibit tubulin assembly. Interestingly, 5-hydroxy flavonol **19** also did not inhibit tubulin assembly in this assay, although the compound arrested cell progression at the G2/M phase. These results

supported the postulate that **6**, **8**, **18**, and **29** directly inhibit tubulin polymerization in a slightly different manner from colchicine binding to tubulin because these compounds only partially competed with colchicine for binding to tubulin.

Table 3. Inhibition of Tubulin Assembly^a and Colchicine Binding.^b

Compound	IC ₅₀ (μM) ± SD	ICB ^c (%) ± SD
6	1.3 ± 0 ^d	61 ± 3
8	1.9 ± 0.3	37 ± 3
9	>20	34 ± 3
16	>20	0
18	1.1 ± 0.1	59 ± 4
19	>20	32 ± 3
20	>20	0
29	1.4 ± 0.1	76 ± 2
CA-4	0.65 ± 0.09	98 ± 0.7

^aThe tubulin assembly assay measured the extent of assembly of 10 μM tubulin after 20 min at 30 °C.

^bTubulin: 0.5 μM, [³H]colchicine: 5 μM, inhibitor: 5 μM. Incubation was for 10 min at 37 °C.

^cInhibition of colchicine binding.

^dSD of 0 indicates same IC₅₀ was obtained in all assays performed with compound **6**. Actual reproducibility of the assay from evaluation of multiple compounds over 30 years is in the range of 15-20%.

2.3.2. Effect of 3-OiPr flavones on Topo I.

One way for a compound to affect the cellular S phase is to inhibit Topo. Topos are enzymes involved in the overwinding or unwinding of DNA and are generally classified into two types, I (Topo I) and II (Topo II). Flavonol **20** was evaluated for Topo I inhibitory activity in a cell-free system using a relaxation assay by simultaneous incubation of supercoiled plasmid DNA as a substrate with purified Topo I in the presence of compound (Figure 9). The assay was performed under a condition where the Topo I could nick supercoiled DNA at almost 100%. In this assay,

compound **20** protected supercoiled DNA from the effects of Topo I in a dose dependent manner, and its inhibitory effect was comparable to that of CPT.

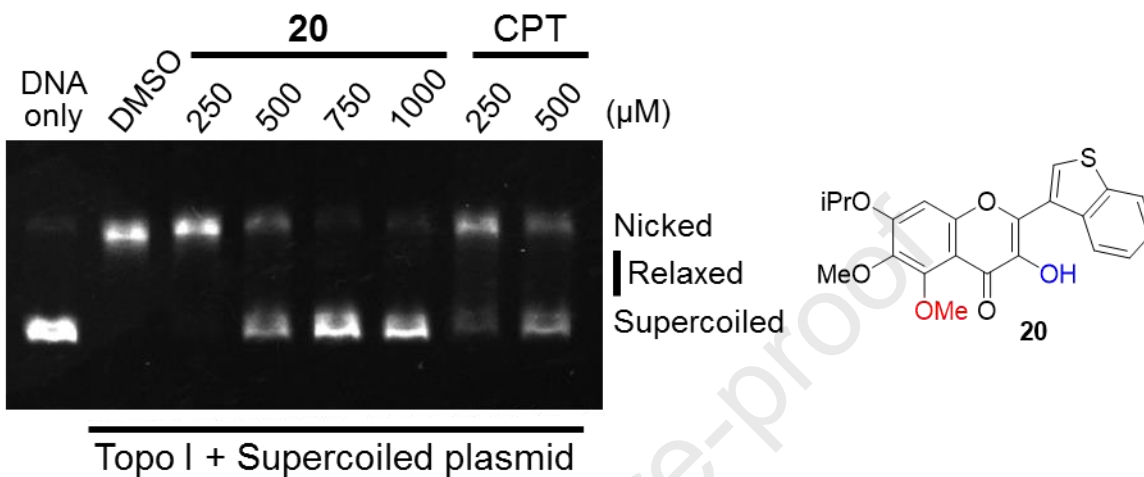


Figure 9. Effects of **20 on Topoisomerase I-mediated DNA Relaxation.**

Supercoiled plasmid DNA was treated with Topo I in the presence of vehicle (DMSO), compound **20** or CPT for 30 min at 37 °C. DNA was separated by 0.8% agarose gel electrophoresis followed by staining with ethidium bromide.

2.4. Summary of SAR findings (Figure 10)

- 1) A ring-B 10 π electron aromatic system was essential for potent antiproliferative activity.
- 2) The ring-B aromaticity influenced the activity order: BT \geq Np > BF >> Ph
- 3) A 3-hydroxy group (R₄ = OH) was crucial for cell cycle arrest at G2/M, while a 5-hydroxy group (R₃ = OH) was important for arrest at G1/S.

For tubulin inhibitory effect (green box in Figure 10),

- i) No substituent at C-3 was preferred rather than hydroxy, alkoxy, or benzoate.
- ii) A 6-methoxy group was important.
- iii) A certain size of 7-alkoxy was necessary.

For the arrest of cell cycle at G1/S (orange box in Figure 10),

- i) A 5-methoxy group was suitable.
- ii) A 7-isopropoxy group was better than a 7-methoxy moiety.

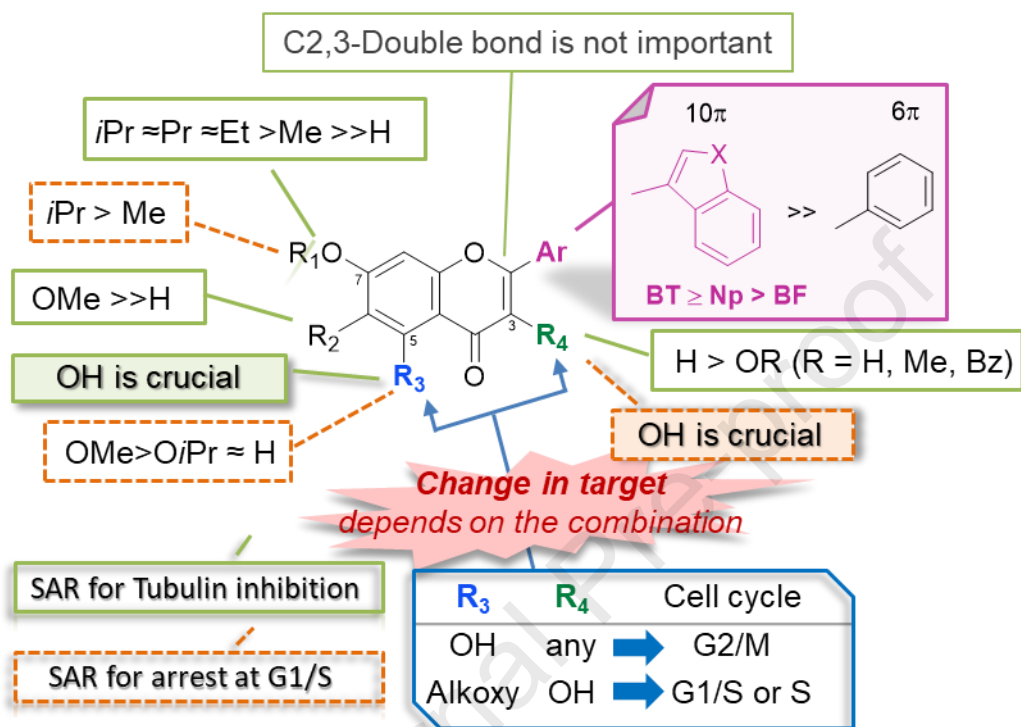


Figure 10. Structure-Activity Relationships of Antiproliferative Flavones.

2.5. Computer Modeling

The theoretical docking form of flavone **6** at the CS in the tubulin dimer was examined by using 1SAO in the Protein Data Bank as a structure of the α/β -tubulin dimer. The modeling indicated that the BT ring-B inserts on the β -tubulin side, and the chromone ring is located in the gap between α - and β -tubulin with adequate room for a bulky isopropyl group (Figure 11). Hydrogen bonds were observed between α Ser178 and the 4-oxo group (2.78 Å) as well as between α Thr179 and the 5-hydroxy group (3.10 Å). Herein, the formation of a hydrogen bond was defined when the distance between the heavy atoms of the hydrogen-bond donor and

acceptor was within 3.9 Å, which is an empirically proposed rule [38, 39]. In the docking simulation, the single-bond rotation is allowed for the calculation of the docking poses and docking scores. That is, note that the hydrogen atoms were not fixed at specific positions. Thus, only the distance between the heavy atoms of the hydrogen-bond donor and acceptor was adopted as the criterion for the formation of a hydrogen bond. The bicyclic ring-B system fit well in the cavity, which might favor hydrophobic contacts. Since no aromatic amino acids were observed around the BT bicycle, the compound is likely stabilized by hydrophobic interactions with the alkyl groups of aliphatic amino acids, such as Leu and Ile.

In addition, the possible docking pose of flavonol **20** at the CPT binding site in Topo I was studied by using 1T81 in the Protein Data Bank as a structure of Topo I. In the model (Figure 12), both BT and chromone rings are located almost parallel to the nucleobase of the DNA. Hydrogen bonding was observed between the 3-hydroxy group of **20** and the guanidino group of Arg364 (2.78 Å). The amino residues, including Thr718, Leu721, and Asn722, close to the chromone moiety could prohibit the insertion of a bulky 5-alkoxy group, such as isopropoxy. This observation may explain why the antiproliferative activity of flavonol **16** was 10-fold weaker than that of **20** (Table 2). In addition, a pocket around C-7 is formed by Ala351, Asn352, Ile427, Met428, Leu429, Asn430, Pro431, and Lys436, which creates an appropriate hydrophobic pocket for a 7-isopropoxy group as found in the four most potent flavonols.

2.6. *In vitro* metabolic stability

A compound's metabolic stability is an important factor in drug discovery and development. Flavone **6** was investigated for microsomal stability using human liver microsomes with the reference compound propranolol, which has a moderate half-life in vivo of 3–6 h. Compound **6**

showed better metabolic stability ($t_{1/2}$ 288.75 min) than propranolol ($t_{1/2}$ 177.69 min) (Figure 13, Table 4). Its estimated half-life in vivo was 4.8 to 9.8 h.

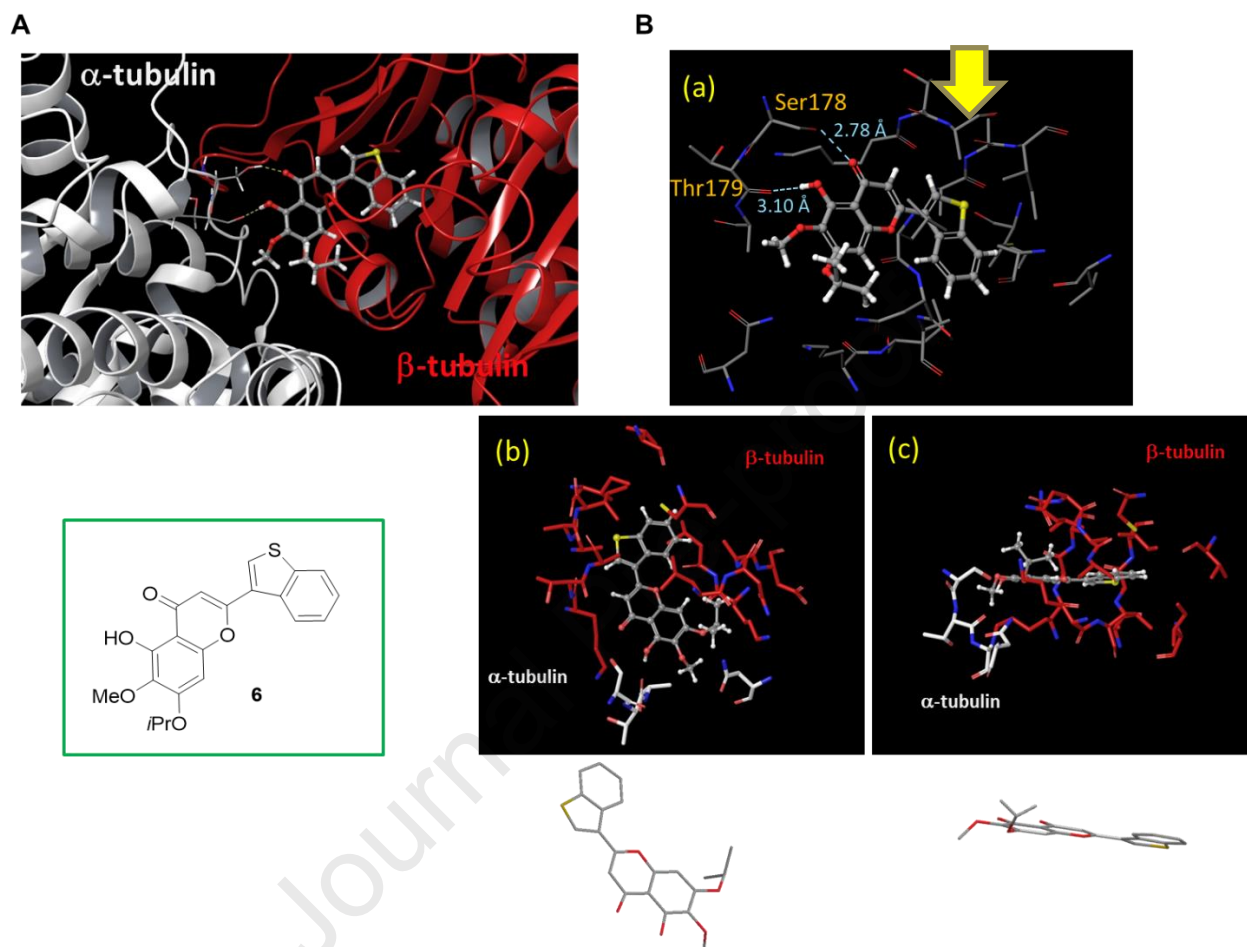


Figure 11. Models for 6 Binding to Tubulin. (A) Docking model of **6** (gray skeleton with oxygen in red and sulfur in yellow) with CS in α - (white) and β -tubulin (red) heterodimer of the tubulin crystal structure (PDB: 1SA0). (B) Docking model of **6** into the CS. (a) Hydrogen bonds calculated to be less than 3.9 Å between amino acid and compounds are represented by dashed lines. Superimposition of docked compound **6** shows hydrogen bonds between α Ser178 (gray skeleton with oxygen in red and nitrogen in blue) and a ketone at C-4 as well as α Thr179 and a 5-hydroxy group. (b), (c) The residues near the ligand within a radius of 4 Å are indicated. (b) View of ligand from upper side. (c) View of ligand from ring plane side. No aromatic amino acid is observed around bicyclic BT ring-B, indicating the compound can be stabilized by hydrophobic interactions with alkyl functions of aliphatic amino acids.

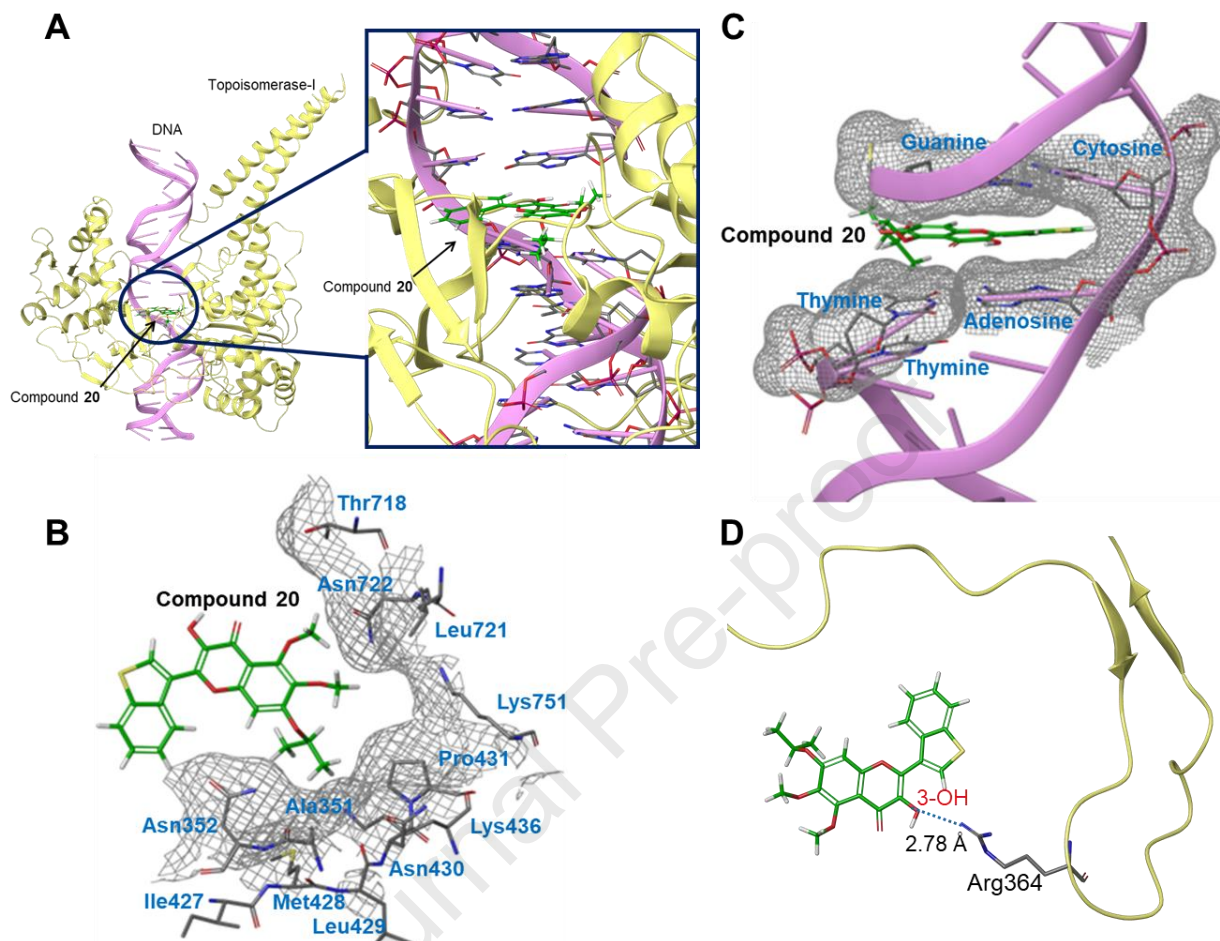


Figure 12. Predicted Docking Models for Compound 20 to Topo I. Docking simulation of compound **20** to Topo I (PDB: 1T8I) was carried out by the calculation program GOLD. The docking score was 59.57. (A) The docking was set so that compound **20** entered within a radius of 10 Å from the coordinates (22.517, -3.374, 27.845). Both BT and chromone rings are located almost parallel to the nucleobase of DNA. (B) Amino residues around chromone moiety on compound **20**. The surface of amino residues is shown as mesh. The presence of Thr718, Leu721, and Asn722 might prohibit the insertion of a bulky group such as isopropyl at C-5. A hydrophobic pocket formed by Ala351, Asn352, Ile427, Met428, Leu429, Asn430, Pro431, and Lys436 around C-7 is an appropriate pocket for a 7-isopropoxy group. (C) Nucleic acid bases around compound **20**. The surface of nucleic acid bases is shown as mesh. The planar chromone and benzothiophene units are in the narrow pocket formed by nucleic acid bases. The bulky 3-alkoxy group might disturb insertion. (D) Hydrogen bonding between 3-OH on compound **20** and guanidino group on Arg364.

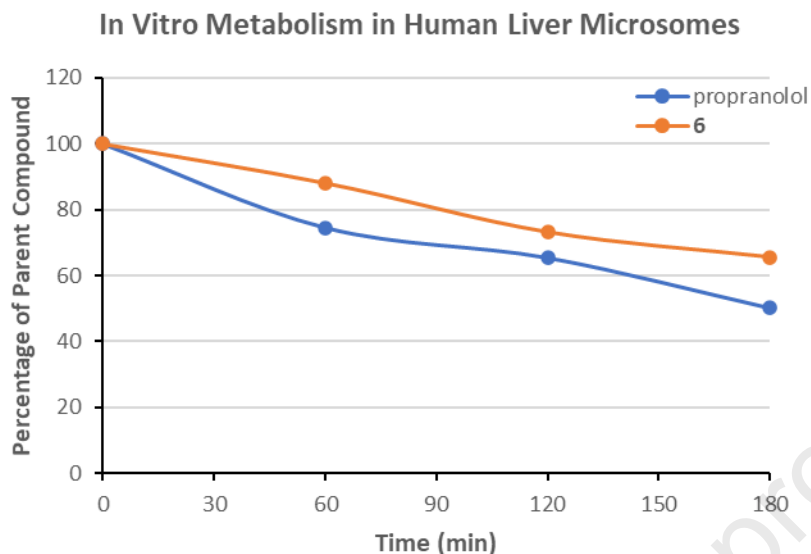


Figure 13. In Vitro Metabolic Stability of Compounds.

Compound **6** was incubated with human liver microsomes at 37 °C. Propranolol was used as a reference compound with a half-life ($t_{1/2}$) of 3 h in this experiment.

Table 4. In Vitro Metabolic Stability of Compounds.

compound	Propranolol	6
In vitro $t_{1/2}$ (min) ^a	177.69	288.75
CL _{int} (mL/min/mg) ^a	0.0078	0.0048

^a Average of three separate experiments with linear regression $R^2 > 0.97$.

3. Conclusions

A new biological scaffold consisting of a hybrid of a chromone and a 10π -aromatic ring-B was designed based on the natural flavone skeleton. The newly synthesized compounds, **1–31**, were evaluated for their antiproliferative activity. Among them, 2-(benzo[*b*]thiophen-3-yl)-5-hydroxy-6-methoxy-7-alkoxyflavones **6**, **8**, and **9** effectively arrested cell cycle progression at the G2/M

phase and displayed significant antiproliferative effects with IC_{50} values of 0.05–0.08 μ M against multiple human cancer cell lines, including an MDR tumor cell line. Furthermore, these compounds inhibited tubulin assembly by binding to the CS in a different manner from that of CA-4. A structure-activity relationship study clearly revealed that a 10π -electron system with high aromaticity as ring-B as well as 5-hydroxy and 7-alkoxy groups are crucial for potent antimitotic activity. Interestingly, the insertion of a 3-hydroxy group and a 5-alkoxy group induced another biological profile. Compound **20** with a 5-methoxy group affected the G1/S phase by inducing DNA damage through inhibition of Topo I, while compound **16** with a 5-isopropoxy group showed similar bioactivity to that of 5-FU, inhibiting DNA replication as well as inducing DNA damage. The detailed SAR correlations from this study are summarized in Figure 10. Docking models of flavone **6** in the CS of tubulin indicated the possibility of hydrogen bonding between a 4-oxo group and a 5-hydroxy group with amino acid residues Ser178 and Thr179, respectively, on α -tubulin. The computational binding model of flavonol **20** with Topo I suggested hydrogen bonding between a 3-hydroxy group and Arg364. Overall, we have discovered a new biological scaffold by connecting a chromone and a 10π -aromatic ring, especially BT, to improve the biological activities of the non-cytotoxic flavonoid chrysin. The different substituent patterns produced three kinds of cell cycle inhibitors, **6**, **16**, and **20**, with different MOAs: inhibition of tubulin assembly, inhibition of DNA replication, and inhibition of Topo I, respectively. Our current study shows that it is possible to find target-selective cell cycle regulators from a natural product modified with an artificial ring that does not occur naturally. Furthermore, the chromone backbone has potential affinity for a variety of proteins, suggesting that target selectivity can be derived by chemical modification.

4. Experimental section

4.1. Chemistry

All commercial chemicals and solvents were used as purchased. ^1H and ^{13}C NMR spectra were recorded on a JEOL JNM-ECA600 spectrometer and JNM-ECS400 spectrometer, with tetramethylsilane (TMS) as an internal standard. Chemical shifts are expressed as δ values in ppm, and apparent scalar coupling constants J are in Hz. High-resolution mass spectrometric data were obtained on a JEOL JMS-700 (FAB) or a JMS-T100TD (DART) mass spectrometer. Analytical and preparative TLC was carried out on precoated silica gel 60F254 and RP-18F254 plates (0.25 or 0.50 mm thickness; Merck). All target compounds were characterized and determined to be at least >95% pure by ^1H -NMR and analytical HPLC (InertSustain C18, GL Science).

4.2. General synthetic procedures for flavones **1**, **4–6**, **12**, **13**, **30**, and **31**

To a solution of the appropriate acetophenones in EtOH (1.0 mL), 50% aq. KOH (1.0 mL) and an appropriate aromatic aldehyde (1.5 eq. mol) were added at 0 °C and stirred at rt. After the reaction was complete by TLC analysis, the mixture was poured into ice-cold 2 N HCl and extracted with EtOAc. The extract was washed with brine, dried over Na_2SO_4 , and concentrated *in vacuo*. The residue was chromatographed twice on silica gel with EtOAc-hexanes, then with CH_2Cl_2 -hexanes as eluent to afford the desired chalcones in 66%–92% yield. Each chalcone was dissolved in DMSO (2.5 mL), and I_2 (0.1 eq. mol) was added. The mixture was stirred at 180 °C for 1.5 or 2 h. The reaction mixture was quenched with ice-cold aqueous 10% $\text{Na}_2\text{S}_2\text{O}_3$ and extracted three times with EtOAc and 5% MeOH/EtOAc. The combined organic layers were

washed with brine, dried over Na₂SO₄, and concentrated *in vacuo*. The residue was purified by silica gel chromatography with EtOAc–hexanes as eluent to afford the desired flavone.

4.2.1. 2-(Benzo[*b*]thiophen-3-yl)-5,7-dimethoxy-4*H*-chromen-4-one (**1**)

Preparation from **33** (57.7 mg, 0.29 mmol) and **35** (72.6 mg, 0.45 mmol) afforded the title compound (78.5 mg, 77%). (Yield calculated from the chalcone intermediate.) ¹H NMR (400 MHz, CDCl₃) δ 3.93 (s, 3H, OMe), 3.98 (s, 3H, OMe), 6.41 (d, 1H, *J* = 2.1 Hz, H-6), 6.58 (d, 1H, *J* = 2.1 Hz, H-8), 6.69 (s, 1H, H-3), 7.43–7.55 (m, 2H, H-5' and H-6'), 7.93 (d, 1H, *J* = 7.9 Hz, H-4'), 8.05 (s, 1H, H-2'), 8.24 (d, 1H, *J* = 7.9 Hz, H-7'); ¹³C NMR (100 MHz, CDCl₃) δ 55.8, 56.5, 92.8, 96.2, 109.4, 111.0, 123.1, 123.3, 125.2, 125.4, 128.6, 129.6, 135.5, 140.6, 157.5, 160.0, 161.0, 164.1, 177.5; HRMS *m/z* [M+H]⁺ calcd for C₁₉H₁₅O₄S, 339.0646; found 339.0658.

4.2.2. 2-(Benzo[*b*]thiophen-3-yl)-5-hydroxy-7-isopropoxy-4*H*-chromen-4-one (**4**)

Preparation from **34** (104.0 mg, 0.69 mmol) and **35** (111.8 mg, 0.69 mmol) afforded the title compound (8.3 mg, 12%) together with 2-(benzo[*b*]thiophen-3-yl)-5,7-diisopropoxy-4*H*-chromen-4-one (53.5 mg, 80%). (Yields were calculated from the chalcone intermediate.) ¹H NMR (400 MHz, CDCl₃) δ 1.40 [d, 6H, *J* = 6.1 Hz, OCH(CH₃)₂], 4.61–4.70 [m, 1H, OCH(CH₃)₂], 6.38 (d, 1H, *J* = 2.1 Hz, H-8), 6.49 (d, 1H, *J* = 2.1 Hz, H-6), 6.67 (s, 1H, H-3), 7.45–7.55 (m, 2H, H-5' and H-6'), 7.95 (d, 1H, *J* = 8.0 Hz, H-4'), 8.10 (s, 1H, H-2'), 8.24 (d, 1H, *J* = 8.0 Hz, H-7'), 12.72 (s, 1H, OH); ¹³C NMR (100 MHz, CDCl₃) δ 21.9, 70.8, 94.0, 99.2, 105.4, 107.6, 123.2, 123.3, 125.4, 125.6, 128.6, 130.7, 135.4, 140.7, 157.8, 162.3, 164.2, 182.3; HRMS *m/z* [M+H]⁺ calcd for C₂₀H₁₇O₄S, 353.0848; found 353.0815.

4.2.3. 2-(Benzo[*b*]thiophen-3-yl)-5,7-diisopropoxy-6-methoxy-4*H*-chromen-4-one (**5**) and 2-(benzo[*b*]thiophen-3-yl)-5-hydroxy-7-isopropoxy-6-methoxy-4*H*-chromen-4-one (**6**)

Preparation from **39** (134.8 mg, 0.48 mmol) and **35** (115.9 mg, 0.72 mmol) afforded **5** (43.4 mg, 35%) and **6** (61.3 mg, 55%). (Yields were calculated from the chalcone intermediate.) **5**: ^1H NMR (400 MHz, CDCl_3) δ 1.40 [d, 6H, $J = 6.7$ Hz, $\text{OCH}(\text{CH}_3)_2$], 1.48 [d, 6H, $J = 5.5$ Hz, $\text{OCH}(\text{CH}_3)_2$], 3.88 (s, 3H, OCH_3), 4.53–4.64 [m, 1H, $\text{OCH}(\text{CH}_3)_2$], 4.65–4.76 [m, 1H, $\text{OCH}(\text{CH}_3)_2$], 6.63 (s, 1H, H-8), 6.77 (s, 1H, H-3), 7.46 (t, 1H, $J = 7.3$ Hz, H-6'), 7.52 (t, 1H, $J = 7.3$ Hz, H-5'), 7.94 (d, 1H, $J = 7.9$ Hz, H-4'), 8.04 (s, 1H, H-2'), 8.23 (d, 1H, $J = 8.0$ Hz, H-7'); ^{13}C NMR (100 MHz, CDCl_3) δ 21.9, 22.4, 60.9, 71.5, 78.1, 97.6, 110.3, 123.1, 123.3, 125.2, 125.3, 128.8, 129.5, 135.6, 140.6, 141.8, 154.7, 156.2, 157.6, 177.1; HRMS (FAB) m/z : $[\text{M}+\text{H}]^+$ calcd for $\text{C}_{24}\text{H}_{25}\text{O}_5\text{S}$, 425.1423, found 425.1427.

6: ^1H NMR (400 MHz, CDCl_3) δ 1.46 [d, 6H, $J = 6.1$ Hz, $\text{OCH}(\text{CH}_3)_2$], 3.91 (s, 3H, OCH_3), 4.66–4.76 [m, 1H, $\text{OCH}(\text{CH}_3)_2$], 6.55 (s, 1H, H-8), 6.67 (s, 1H, H-3), 7.47 (t, 1H, $J = 7.6$ Hz, H-6'), 7.51–7.57 (m, 1H, H-5'), 7.95 (d, 1H, $J = 7.9$ Hz, H-4'), 8.10 (s, 1H, H-2'), 8.22 (d, 1H, $J = 8.6$ Hz, H-7'), 12.67 (s, 1H, OH); ^{13}C NMR (100 MHz, CDCl_3) δ 22.0, 60.7, 92.4, 106.1, 107.4, 123.2, 123.2, 125.4, 125.6, 128.6, 130.6, 135.4, 140.7, 153.3, 153.5, 157.6, 160.6, 182.5; HRMS m/z $[\text{M}+\text{H}]^+$ calcd for $\text{C}_{21}\text{H}_{19}\text{O}_5\text{S}$, 383.0953; found 383.0931.

4.2.4. 5-Hydroxy-7-isopropoxy-6-methoxy-2-(naphthalen-1-yl)-4*H*-chromen-4-one (**12**)

Preparation from **39** (42.0 mg, 0.15 mmol) and **37** (0.03 mL, 0.22 mmol) afforded **12** (13.1 mg, 28%). (Yield calculated from the chalcone intermediate.) ^1H NMR (400 MHz, CDCl_3) δ 1.43 [6H, d, $J = 6.1$ Hz, $\text{OCH}(\text{CH}_3)_2$], 3.92 (3H, s, OCH_3), 4.60–4.70 [1H, m, $\text{OCH}(\text{CH}_3)_2$], 6.51

(1H, s, H-8), 6.54 (1H, s, H-3), 7.56–7.62 (3H, m, H-3', H-6' and H-7'), 7.74 (dd, 1H, $J = 1.2$ Hz, 7.3 Hz, H-2'), 7.93–7.99 (m, 1H, H-8'), 8.03 (1H, d, $J = 8.0$ Hz, H-4'), 8.07–8.13 (1H, m, H-5'), 12.67 (1H, s, OH); ^{13}C NMR (150 MHz, CDCl_3) δ 21.9, 60.7, 71.7, 92.5, 106.0, 111.0, 124.7, 125.1, 126.7, 127.6, 128.0, 128.8, 130.28, 130.32, 131.7, 133.6, 133.7, 153.5, 153.8, 157.6, 165.8, 182.6; HRMS (FAB) m/z : $[\text{M}+\text{H}]^+$ calcd for $\text{C}_{23}\text{H}_{21}\text{O}_5$, 377.1389, found 377.1395.

4.2.5. 2-(Benzo[*b*]thiophen-3-yl)-7-isopropoxy-4*H*-chromen-4-one (**13**)

The treatment of **41** (353.2 mg, 1.82 mmol) with **35** (442.4 mg, 2.73 mmol) produced the related chalcone (386.2 mg), of which 159.0 mg (0.47 mmol) was used for the cyclization to give **13** (152.1 mg, 96%). ^1H NMR (400 MHz, CDCl_3) δ 1.43 [6H, d, $J = 6.7$ Hz, $\text{OCH}(\text{CH}_3)_2$], 4.68–4.74 [1H, m, $\text{OCH}(\text{CH}_3)_2$], 6.76 (1H, s, H-3), 6.95 (1H, d, $J = 1.8$ Hz, H-8), 6.98 (1H, dd, $J = 9.0$ and 2.3 Hz, H-6), 7.45–7.54 (2H, m, H-5', H-6'), 8.08 (1H, s, H-2'), 8.16 (1H, d, $J = 9.2$ Hz, H-5), 8.26 (1H, d, $J = 8.3$ Hz, H-4'), 7.95 (1H, d, $J = 7.2$ Hz, H-7'); ^{13}C NMR (100 MHz, CDCl_3) δ 21.9, 70.8, 101.9, 109.4, 115.3, 117.6, 123.1, 123.3, 125.3, 125.4, 127.2, 129.0, 129.9, 135.6, 140.7, 158.1, 159.7, 162.7, 177.7; HRMS m/z $[\text{M}+\text{H}]^+$ calcd for $\text{C}_{20}\text{H}_{17}\text{O}_3\text{S}$, 337.0898; found 337.0895.

4.2.6. 5,7-Diisopropoxy-6-methoxy-2-phenyl-4*H*-chromen-4-one (**30**) and 5-hydroxy-7-isopropoxy-6-methoxy-2-phenyl-4*H*-chromen-4-one (**31**)

Preparation from **39** (26.4 mg, 0.09 mmol) and benzaldehyde (0.02 mL, 0.20 mmol) afforded **30** (11.7 mg, 48%) and **31** (4.2 mg, 19%). (Yields were calculated from the chalcone intermediate.) **30**: ^1H NMR (400 MHz, CDCl_3) δ 1.38 [6H, d, $J = 6.0$ Hz, $\text{OCH}(\text{CH}_3)_2$], 1.47 [6H, d, $J = 6.4$ Hz, $\text{OCH}(\text{CH}_3)_2$], 3.87 (3H, s, OCH_3), 4.52–4.62 [1H, m, $\text{OCH}(\text{CH}_3)_2$], 4.64–4.74

[1H, m, OCH(CH₃)₂], 6.62 (1H, s, H-8), 6.78 (1H, s, H-3), 7.47–7.53 (3H, m, H-3', H-4' and H-5'), 7.85–7.89 (2H, m, H-2' and H-6'); ¹³C NMR (100 MHz, CDCl₃) δ 21.9, 22.4, 60.9, 71.5, 78.0, 97.6, 108.4, 126.0, 128.9, 131.1, 131.7, 150.6, 154.7, 156.1, 177.3; HRMS *m/z* [M+H]⁺ calcd for C₂₂H₂₅O₅, 369.1702; found 369.1680.

31: ¹H NMR (400 MHz, CDCl₃) δ 1.45 [6H, d, *J* = 6.1 Hz, OCH(CH₃)₂], 3.89 (3H, s, OCH₃), 4.63–4.74 [1H, m, OCH(CH₃)₂], 6.54 (1H, s, H-8), 6.66 (1H, s, H-3), 7.49–7.58 (3H, m, H-3', H-4' and H-5'), 7.86–7.92 (2H, m, H-2' and H-6'), 12.64 (1H, s, OH); ¹³C NMR (150 MHz, CDCl₃) δ 21.9, 60.7, 71.7, 92.5, 105.6, 106.0, 126.3, 129.1, 131.4, 131.8, 133.5, 153.3, 153.4, 157.5, 163.9, 182.7; HRMS (FAB) *m/z*: [M+H]⁺ calcd for C₁₉H₁₉O₅ 327.1232, found 327.1239.

4.3. 2-(Benzofuran-3-yl)-5-hydroxy-7-isopropoxy-6-methoxy-4H-chromen-4-one (**11**)

To a solution of **39** (47.8 mg, 0.17 mmol) in DMF (1.5 mL), Ba(OH)₂ (90.8 mg, 0.53 mmol) and **36** (46.2 mg, 0.316 mmol) were added and stirred at 90 °C for 1.5 h. After the reaction was complete by TLC analysis, the mixture was poured into ice-cold 1 N HCl and extracted with EtOAc. The extract was washed with brine, dried over Na₂SO₄, and concentrated *in vacuo*. The residue was chromatographed twice on silica gel with EtOAc-hexanes, then with CH₂Cl₂-hexanes as eluent to afford the related chalcone (44.1 mg, 64%), which was dissolved in DMSO (1.0 mL), and I₂ (2.7 mg, 0.01 mmol) was added. The mixture was stirred at 180 °C for 7 h. The reaction mixture was quenched with ice-cold aqueous 10% Na₂S₂O₃ and extracted three times with EtOAc and 5% MeOH/EtOAc. The combined organic layers were washed with brine, dried over Na₂SO₄, and concentrated *in vacuo*. The residue was purified by silica gel chromatography with EtOAc-hexanes as eluent to afford **11** (13.1 mg, 28%) together with 2-(benzofuran-3-yl)-5,7-diisopropoxy-6-methoxy-4H-chromen-4-one (2.1 mg, 5%). ¹H NMR (400 MHz, CDCl₃)

δ 1.47 [d, 6H, $J = 6.1$ Hz, OCH(CH₃)₂], 3.90 (s, 3H, OCH₃), 4.66–4.77 [m, 1H, OCH(CH₃)₂], 6.52 (s, 1H, H-8), 6.66 (s, 1H, H-3), 7.40–7.48 (m, 2H, H-5' and H-6'), 7.59–7.64 (m, 1H, H-4'), 7.92–7.98 (m, 1H, H-7'), 8.29 (s, 1H, H-2'), 12.65 (s, 1H, OH); ¹³C NMR (100 MHz, CDCl₃) δ 21.9, 60.7, 71.7, 92.4, 106.0, 106.3, 112.3, 115.3, 120.8, 123.2, 124.4, 125.8, 133.6, 146.4, 153.1, 153.5, 155.9, 157.5, 159.0, 182.2; HRMS m/z [M+H]⁺ calcd for C₂₁H₁₉O₆, 367.1182; found 367.1153.

4.4. 2-(Benzo[b]thiophen-3-yl)-5-hydroxy-7-methoxy-4H-chromen-4-one (**2**) and 2-(benzo[b]thiophen-3-yl)-5,7-hydroxy-4H-chromen-4-one (**3**)

To a solution of **1** (78.5 mg, 0.23 mmol) in CH₂Cl₂ (2.0 mL), BBr₃ (2.1 ml, 2.1 mmol, 1.0 M solution in CH₂Cl₂) was added at 0 °C. The mixture was warmed to rt and stirred at 45 °C for 20 h. After addition of water, the reaction mixture was extracted three times with CH₂Cl₂. The combined organic layers were washed with brine, dried over Na₂SO₄, and concentrated *in vacuo*. The residue was chromatographed on silica gel, eluting with EtOAc-hexanes to yield **2** (19.6 mg, 26%) and **3** (24.5 mg, 34%).

2: ¹H NMR (400 MHz, CDCl₃) δ 3.90 (s, 3H, OMe), 6.41 (d, 1H, $J = 2.1$ Hz, H-6), 6.51 (d, 1H, $J = 2.1$ Hz, H-8), 6.67 (s, 1H, H-3), 7.45–7.56 (m, 2H, H-5' and H-6'), 7.95 (d, 1H, $J = 7.9$ Hz, H-4'), 8.10 (s, 1H, H-2'), 8.23 (d, 1H, $J = 8.6$ Hz, H-7'), 12.75 (s, 1H, OH); ¹³C NMR (100 MHz, CDCl₃) δ 55.9, 92.7, 98.2, 105.7, 107.6, 123.2, 123.2, 125.4, 125.6, 128.5, 130.8, 135.4, 140.7, 157.8, 160.7, 162.3, 165.7, 182.4; HRMS m/z [M+H]⁺ calcd for C₁₈H₁₃O₄S, 325.0535; found 325.0498.

3: ¹H NMR (400 MHz, DMSO-*d*₆) δ 6.26 (d, 1H, $J = 2.1$ Hz, H-6), 6.56 (d, 1H, $J = 2.1$ Hz, H-8), 6.85 (s, 1H, H-3), 7.50–7.62 (m, 2H, H-5' and H-6'), 8.17 (d, 1H, $J = 8.0$ Hz, H-4'), 8.33 (d,

1H, $J = 8.0$ Hz, H-7'), 8.75 (s, 1H, H-2'), 10.94 (s, 1H, OH), 12.87 (s, 1H, OH); ^{13}C NMR (100 MHz, DMSO- d_6) δ 94.6, 99.6, 104.5, 107.1, 124.0, 125.9, 126.3, 127.9, 133.7, 135.6, 140.6, 157.9, 161.2, 162.0, 165.0, 182.1; HRMS m/z $[\text{M}+\text{H}]^+$ calcd for $\text{C}_{17}\text{H}_{11}\text{O}_4\text{S}$, 311.0333; found 311.0375.

4.5. 2-(Benzo[b]thiophen-3-yl)-5,7-dihydroxy-6-methoxy-4H-chromen-4-one (7)

A flask containing AlCl_3 (8.9 mg, 0.067 mmol) was cooled at 0°C under a N_2 atmosphere. A solution of **6** (6.0 mg, 0.016 mmol) in CH_2Cl_2 (1.5 mL) was added. The mixture was warmed to rt and stirred for 1.5 h. The reaction was quenched with sat. NH_4Cl aq. (10.0 mL), extracted with CH_2Cl_2 , subsequently with EtOAc. The combined organic layers were washed with brine, dried over Na_2SO_4 , and concentrated in vacuo. The residue was chromatographed on silica gel, eluting with EtOAc-hexanes to yield **7** (2.0 mg, 37%). ^1H NMR (400 MHz, CDCl_3) δ 4.05 (s, 3H, OCH_3), 6.57 (s, 1H, OH), 6.62 (s, 1H, H-8), 6.65 (s, 1H, H-3), 7.46 (t, 1H, $J = 7.3$ Hz, H-6'), 7.49-7.56 (m, 1H, H-5'), 7.93 (d, 1H, $J = 7.9$ Hz, H-4'), 8.09 (s, 1H, H-2'), 8.22 (d, 1H, $J = 8.0$ Hz, H-7'), 13.01 (s, 1H, OH); ^{13}C NMR (100 MHz, CDCl_3) δ 61.0, 93.5, 106.0, 107.0, 123.3, 123.3, 125.5, 125.7, 128.5, 130.5, 130.9, 135.4, 140.7, 152.3, 153.3, 155.3, 160.9, 183.0; HRMS m/z $[\text{M}+\text{H}]^+$ calcd for $\text{C}_{18}\text{H}_{13}\text{O}_5\text{S}$, 341.0484; found 341.0437.

4.6. 2-(Benzo[b]thiophen-3-yl)-5-hydroxy-6-methoxy-7-propoxy-4H-chromen-4-one (8)

To a solution of **7** (15.9 mg, 0.05 mmol) in acetone (2.0 mL), K_2CO_3 (10.4 mg, 0.08 mmol) and PrI (0.005 mL, 0.05 mmol) were added. The mixture was refluxed for 5 h. After cooling, solid K_2CO_3 was removed through cotton filtration, and the volatile solvent was removed *in vacuo*. The residue was chromatographed on silica gel, eluting with EtOAc-hexanes to yield **8** (10.9 mg,

62%) and residual **7** (3.6 mg, 23%). ^1H NMR (400 MHz, CDCl_3) δ 1.11 (3H, t, $J = 7.3$ Hz, $\text{OCH}_2\text{CH}_2\text{CH}_3$), 1.89–2.00 (2H, m, $\text{OCH}_2\text{CH}_2\text{CH}_3$), 3.93 (3H, s, OCH_3), 4.09 (2H, t, $J = 6.4$ Hz, $\text{OCH}_2\text{CH}_2\text{CH}_3$), 6.56 (1H, s, H-8), 6.68 (1H, s, H-3), 7.45–7.57 (2H, m, H-5' and H-6'), 7.96 (1H, d, $J = 6.7$ Hz, H-4'), 8.10 (1H, s, H-2'), 8.23 (1H, d, $J = 8.0$ Hz, H-7'), 12.67 (1H, s, OH); ^{13}C NMR (100 MHz, CDCl_3) δ 10.6, 22.4, 61.0, 70.9, 91.4, 106.3, 107.5, 123.3, 123.6, 125.5, 125.7, 128.6, 130.7, 133.0, 135.5, 140.7, 153.3, 153.4, 158.7, 160.7, 182.6; HRMS m/z $[\text{M}+\text{H}]^+$ calcd for $\text{C}_{21}\text{H}_{19}\text{O}_5\text{S}$, 383.0953; found 383.0913.

4.7. 2-(Benzo[b]thiophen-3-yl)-7-ethoxy-5-hydroxy-6-methoxy-4H-chromen-4-one (**9**)

A similar procedure to that described above was performed using **7** (12.5 mg, 0.04 mmol), K_2CO_3 (8.0 mg, 0.06 mmol), and EtI (0.003 ml, 0.04 mmol) to generate **9** (7.6 mg, 56%) together with residual **7** (2.5 mg, 20%). ^1H NMR (400 MHz, CDCl_3) δ 1.54 (3H, t, $J = 7.0$ Hz, OCH_2CH_3), 3.94 (3H, s, OCH_3), 4.17–4.25 (2H, m, OCH_2CH_3), 6.56 (1H, s, H-8), 6.68 (1H, s, H-3), 7.45–7.57 (2H, m, H-5' and H-6'), 7.96 (1H, d, $J = 8.0$, H-4'), 8.10 (1H, s, H-2'), 8.23 (1H, d, $J = 8.0$ Hz, H-7'), 12.68 (1H, s, OH); ^{13}C NMR (150 MHz, CDCl_3) δ 14.6, 60.8, 64.9, 91.3, 106.2, 107.4, 123.20, 123.23, 125.5, 125.6, 128.6, 130.6, 133.0, 135.4, 140.7, 153.2, 153.3, 158.4, 160.6, 182.6; HRMS (FAB) m/z : $[\text{M}+\text{H}]^+$ calcd for $\text{C}_{20}\text{H}_{17}\text{O}_5\text{S}$ 369.0797, found 369.0812.

4.8. 2-(Benzo[b]thiophen-3-yl)-5-hydroxy-6,7-dimethoxy-4H-chromen-4-one (**10**)

To a solution of **7** (10.5 mg, 0.03 mmol) in acetone (2.0 mL), K_2CO_3 (6.6 mg, 0.05 mmol) and Me_2SO_4 (0.004 ml, 0.04 mmol) were added. The mixture was refluxed for 11 h. After cooling to rt, the reaction mixture was quenched with water (10 mL) and acidified with 2 N HCl. The mixture was extracted three times with EtOAc. The combined organic layers were washed with

brine, dried over Na_2SO_4 , and concentrated *in vacuo*. The residue was chromatographed on silica gel, eluting with EtOAc-hexanes to yield **10** (6.5 mg, 85% based on recovery of starting material). ^1H NMR (400 MHz, CDCl_3) δ 3.95 (3H, s, OMe), 4.00 (3H, s, OMe), 6.58 (1H, s, H-8), 6.69 (1H, s, H-3), 7.46-7.58 (2H, m, H-5' and H-6'), 7.96 (1H, d, $J = 7.4$ Hz, H-4'), 8.11 (1H, s, H-2'), 8.24 (1H, d, $J = 7.3$ Hz, H-7'), 12.71 (1H, s, OH); ^{13}C NMR (150 MHz, CDCl_3) δ 56.4, 60.9, 90.6, 106.4, 107.5, 123.19, 123.23, 125.5, 125.6, 128.5, 130.7, 132.8, 135.4, 140.7, 153.2, 153.4, 159.0, 160.7, 182.6; HRMS (FAB) m/z : $[\text{M}+\text{H}]^+$ calcd for $\text{C}_{19}\text{H}_{15}\text{O}_5\text{S}$ 355.0640, found 355.0624.

4.9. 2-(Benzo[b]thiophen-3-yl)-5,7-diisopropoxy-6-methoxychroman-4-one (**28**)

The chalcone (14.2 mg, 0.03 mmol) produced from **39** and **35** as described above was dissolved in MeOH (2.7 mL), and the solution was cooled to 0 °C, then 2 N HCl (0.38 mL) was added. The mixture was refluxed for 6 h. After cooling to rt, the reaction mixture was extracted three times with EtOAc. The combined organic layers were washed with brine, dried over Na_2SO_4 , and concentrated *in vacuo*. The residue was chromatographed on silica gel, eluting with CH_2Cl_2 to yield **28** (7.9 mg, 56%). ^1H NMR (400 MHz, CDCl_3) δ 1.32 [3H, d, $J = 6.1$ Hz, $\text{OCH}(\text{CH}_3)_2$], 1.38 [3H, d, $J = 6.1$ Hz, $\text{OCH}(\text{CH}_3)_2$], 1.41 [3H, d, $J = 4.3$ Hz, $\text{OCH}(\text{CH}_3)_2$], 1.42 [3H, d, $J = 4.3$ Hz, $\text{OCH}(\text{CH}_3)_2$], 3.00 (2H, dd, $J = 16.5$ Hz and 3.0 Hz, H-3), 3.78 (3H, s, OMe), 4.52-4.61 [2H, m, $\text{OCH}(\text{CH}_3)_2$], 5.79 (1H, dd, $J = 12.2$ Hz and 3.0 Hz, H-2), 6.31 (1H, s, H-8), 7.37-7.46 (2H, m, 5'-H and H-6'), 7.54 (1H, s, H-2'), 7.90 (1H, d, $J = 8.5$ Hz, H-4'), 7.93 (1H, d, $J = 7.3$ Hz, H-7'); ^{13}C NMR (100 MHz, CDCl_3) δ 21.9, 22.4, 22.6, 43.8, 60.7, 71.2, 74.3, 97.5, 109.8, 122.2, 123.0, 124.5, 124.6, 124.8, 133.5, 137.0, 138.8, 140.8, 152.4, 157.9, 159.4, 188.9; HRMS (FAB) m/z : $[\text{M}+\text{H}]^+$ calcd for $\text{C}_{24}\text{H}_{27}\text{O}_5\text{S}$ 427.1579, found 427.1578.

4.10. 2-(Benzo[b]thiophen-3-yl)-5-hydroxy-7-isopropoxy-6-methoxychroman-4-one (**29**)

The same procedure as described above for **7** was performed using **28** (19.2 mg, 0.05 mmol) and AlCl₃ (18.0 mg, 0.14 mmol) to produce **29** (3.3 mg, 19%). ¹H NMR (400 MHz, CDCl₃) δ 1.37 [3H, d, *J* = 6.1 Hz, OCH(CH₃)₂], 1.40 [3H, d, *J* = 6.1 Hz, OCH(CH₃)₂], 3.03 (1H, dd, *J* = 17.1 Hz and 3.0 Hz, H-3), 3.30 (1H, dd, *J* = 17.1 Hz and 12.2 Hz, H-3), 3.82 (3H, s, OMe), 4.54–4.65 [2H, m, OCH(CH₃)₂], 5.82 (1H, dd, *J* = 12.2 Hz and 3.0 Hz, H-2), 6.10 (1H, s, H-8), 7.38–7.47 (2H, m, 5'-H and H-6'), 7.54 (1H, s, H-2'), 7.91 (2H, d, *J* = 7.9 Hz, H-4' and H-7'), 11.8 (1H, s, OH); ¹³C NMR (100 MHz, CDCl₃) δ 21.96, 22.02, 41.6, 60.7, 71.5, 74.6, 93.2, 103.0, 122.1, 123.1, 124.6, 124.7, 125.0, 131.4, 133.2, 136.8, 140.8, 155.5, 158.2, 159.7, 195.9; HRMS (FAB) *m/z*: [M]⁺ calcd for C₂₁H₂₀O₅S 384.1031, found 384.1015.

4.11. 2-Acetyl-3,5-diisopropoxy-4-methoxyphenyl benzo[b]thiophene-3-carboxylate (**43**)

To a solution of **39** (235.5 mg, 0.84 mmol) in CH₂Cl₂ (5.0 mL), **42** (276.0 mg, 1.55 mmol), *N,N*-dimethyl-4-aminopyridine (DMAP, 51.9 mg, 0.42 mmol), and 1-ethyl-3-(dimethylaminopropyl)carbodiimide (EDCI, 0.37 ml, 2.10 mmol) were added. The mixture was stirred at rt for 3 h under N₂. The reaction was quenched with sat. NaHCO₃ aq. and CH₂Cl₂ and then stirred for 15 min. The mixture was extracted three times with CH₂Cl₂. The combined organic layers were washed with brine, dried over Na₂SO₄, and concentrated *in vacuo*. The residue was chromatographed on silica gel, eluting with EtOAc–hexanes to yield **43** (362.0 mg, 98%).

¹H NMR (400 MHz, CDCl₃) δ 1.27 [6H, d, *J* = 6.0 Hz, OCH(CH₃)₂], 1.40 [6H, d, *J* = 6.0 Hz, OCH(CH₃)₂], 2.53 (3H, s, COCH₃), 3.88 (3H, s, OMe), 4.65–4.52 (2H, m, OCH(CH₃)₂), 6.58

(1H, s, 5-H), 7.53–7.41 (2H, m, 5'-H and 6'-H), 7.90 (1H, d, $J = 8.4$ Hz, 4'-H), 8.60–8.56 (2H, m, 2'-H and 7'-H). ^{13}C NMR (150 MHz, CDCl_3) δ 22.0, 22.6, 32.1, 60.7, 71.4, 104.7, 122.5, 123.3, 124.6, 125.3, 125.7, 125.8, 136.7, 138.6, 140.0, 141.0, 142.6, 149.8, 153.4, 160.8, 200.4; HRMS (FAB) m/z : $[\text{M}]^+$ calcd for $\text{C}_{24}\text{H}_{27}\text{O}_6\text{S}$ 443.1528, found 443.1553.

4.12. 2-(2-Bromoacetyl)-3,5-diisopropoxy-4-methoxyphenyl benzo[*b*]thiophene-3-carboxylate (**44**)

To a solution of **43** (326.6 mg, 0.74 mmol) in THF (7.0 mL), trimethylphenylammonium tribromide (276.8 mg, 0.74 mmol) was added, and the mixture was stirred at rt for 1 h under N_2 . The reaction was quenched with water. After extraction three times with EtOAc, the combined organic layers were washed with brine, dried over Na_2SO_4 , and concentrated *in vacuo*. The residue was chromatographed on silica gel, eluting with CH_2Cl_2 –hexanes to yield **44** (188.8 mg, 49%) together with an undesired dibromoacetyl compound (84 mg, 22%) and residual **43** (94.5 mg, 29%). ^1H NMR (400 MHz, CDCl_3) δ 1.27 [6H, d, $J = 6.0$ Hz, $\text{OCH}(\text{CH}_3)_2$], 1.41 [6H, d, $J = 6.0$ Hz, $\text{OCH}(\text{CH}_3)_2$], 3.88 (3H, s, OMe), 4.53 (2H, s, COCH_2Br), 4.68–4.55 [2H, m, $\text{OCH}(\text{CH}_3)_2$], 6.64 (1H, s, 5-H), 7.53–7.41 (2H, m, 5'-H and 6'-H), 7.90 (1H, d, $J = 8.0$ Hz, 4'-H), 8.60–8.55 (2H, m, 2'-H and 7'-H); ^{13}C NMR (150 MHz, CDCl_3) δ 22.0, 22.6, 36.9, 60.7, 71.5, 104.9, 119.5, 122.5, 124.6, 125.3, 125.5, 125.7, 136.7, 138.9, 139.9, 140.7, 143.6, 150.0, 154.4, 160.6, 192.7; HRMS (FAB) m/z : $[\text{M}]^+$ calcd for $\text{C}_{24}\text{H}_{26}\text{BrO}_6\text{S}$ 521.0633, found 521.0618.

4.23. 2-[2-(Benzoyloxy)acetyl]-3,5-diisopropoxy-4-methoxyphenyl benzo[*b*]thiophene-3-carboxylate (**45**)

To a solution of **44** (191.2 mg, 0.37 mmol) in CH₃CN (4.0 mL), potassium benzoate (118.1 mg, 0.74 mmol) was added. The mixture was refluxed for 30 min. The remaining solid was removed through cotton filtration. After evaporation of the solvent in vacuo, the residue was partitioned with CH₂Cl₂ and sat. Na₂CO₃ aq. The organic layer was washed with water, dried over Na₂SO₄, and concentrated *in vacuo*. The residue was chromatographed on silica gel, eluting with EtOAc–hexanes to yield **45** (115.2 mg, 56%). ¹H NMR (400 MHz, CDCl₃) δ 1.32 [6H, d, *J* = 6.4 Hz, OCH(CH₃)₂], 1.42 [6H, d, *J* = 6.4 Hz, OCH(CH₃)₂], 3.84 (3H, s, OMe), 4.60–4.72 [2H, m, OCH(CH₃)₂], 5.37 (2H, s, COCH₂O), 6.68 (1H, s, H-8), 7.35–7.55 (5H, m, H-5', H-6', H-3'', H-4'' and H-5''), 7.88 (1H, d, *J* = 8.0 Hz, H-4'), 7.98–8.02 (2H, m, H-2'' and H-7''), 8.60 (1H, d, *J* = 8.0 Hz, H-7'), 8.62 (1H, s, H-2'). ¹³C NMR (150 MHz, CDCl₃) δ 22.0, 22.5, 60.7, 69.6, 71.5, 77.1, 105.2, 119.3, 122.5, 124.7, 125.1, 125.57, 125.63, 128.3, 129.7, 129.9, 133.0, 136.8, 139.0, 139.9, 140.7, 143.8, 150.3, 154.2, 160.6, 165.8, 194.8; HRMS (FAB) *m/z*: [M]⁺ calcd for C₃₁H₃₁O₈S 563.1740, found 563.1729.

4.24. 2-(Benzo[*b*]thiophen-3-yl)-5,7-diisopropoxy-6-methoxy-4-oxo-4*H*-chromen-3-yl benzoate (**14**)

To a suspension of 60% NaH (19.1 mg, 0.48 mmol, washed with hexanes) in THF (1.0 mL), a solution of **45** (89.9 mg, 0.16 mmol) in THF (3.0 mL) was added at 0 °C. The mixture was heated at 65 °C for 0.25 h under N₂. After cooling to 0 °C, the reaction was quenched with water and acidified with 2 N HCl. After extraction with EtOAc and 5% MeOH/EtOAc, the combined organic layers were washed with brine, dried over Na₂SO₄, and concentrated *in vacuo*. The residue was roughly purified using chromatography on silica gel eluting with EtOAc–hexanes to yield **46**, which was dissolved in AcOH (1.5 mL). Then, NaOAc (26.6 mg, 0.32 mmol) was

added to the solution. The mixture was heated at 100 °C for 4 h and partitioned between EtOAc and water. The organic layer was washed with brine, dried over Na₂SO₄, and concentrated *in vacuo*. The residue was chromatographed on silica gel eluting with EtOAc–hexanes to afford **14** (32.5 mg, 2 steps 37%). ¹H NMR (400 MHz, CDCl₃) δ 1.37 [6H, d, *J* = 6.4 Hz, OCH(CH₃)₂], 1.47 [6H, d, *J* = 6.4 Hz, OCH(CH₃)₂], 3.88 (3H, s, OMe), 4.60–4.72 [2H, m, OCH(CH₃)₂], 6.76 (1H, s, H-8), 7.40–7.62 (5H, m, H-5', H-6', H-3'', H-4'' and H-6''), 7.89 (1H, d, *J* = 8.0 Hz, H-4'), 7.99 (1H, s, H-2'), 8.09–8.14 (2H, m, H-2'' and H-7''), 8.17 (1H, d, *J* = 8.0 Hz, H-7'); ¹³C NMR (150 MHz, CDCl₃) δ 21.9, 22.4, 60.9, 71.6, 77.9, 97.4, 113.4, 122.8, 123.8, 125.08, 125.12, 125.3, 128.5, 128.7, 130.6, 130.8, 133.6, 134.1, 136.7, 139.8, 141.9, 151.03, 151.09, 154.1, 156.4, 164.0, 170.2; HRMS (FAB) *m/z*: [M+H]⁺ calcd for C₃₁H₂₉O₇S 545.1634, found 545.1626.

4.25. *2-(Benzo[b]thiophen-3-yl)-5-hydroxy-7-isopropoxy-6-methoxy-4-oxo-4H-chromen-3-yl benzoate (15)*

To a solution of **14** (4.7 mg, 0.009 mmol) in CH₂Cl₂ (1.0 mL), TiCl₄ (2.6 μL, 0.026 mmol, 1.0 M solution in CH₂Cl₂) was added at 0 °C. The mixture was warmed at rt and stirred. Additional TiCl₄ (2.6 μL, 0.026 mmol and 5.6 μL, 0.051 mmol, 1.0 M solution in CH₂Cl₂) was added separately at 0 °C after 4 h and 14 h. The mixture was continuously stirred at rt for 4 h. After addition of water, the mixture was extracted three times with CH₂Cl₂. The combined organic layers were washed with brine, dried over Na₂SO₄, and concentrated *in vacuo*. The residue was purified using chromatography on silica gel eluting with CH₂Cl₂–hexanes to yield **15** (3.5 mg, 81%). ¹H NMR (400 MHz, CDCl₃) δ 1.47 [6H, d, *J* = 6.0 Hz, OCH(CH₃)₂], 3.91 (3H, s, OMe), 4.70–4.74 [1H, m, OCH(CH₃)₂], 6.58 (1H, s, H-8), 7.42–7.56 (4H, m, H-5', H-6', H-3'' and H-5''), 7.60–7.66 (1H, m, H-4''), 7.91 (1H, d, *J* = 8.0 Hz, 4'-H), 8.01 (1H, s, H-2'), 8.12–8.20 (3H,

m, H-7', H-2'' and H-6''), 12.10 (1H, s, OH); ^{13}C NMR (150 MHz, CDCl_3) δ 21.9, 60.8, 71.9, 92.5, 106.1, 122.9, 123.7, 124.8, 125.4, 128.1, 128.7, 130.5, 131.9, 132.0, 133.8, 134.1, 136.4, 139.8, 152.7, 153.3, 153.9, 158.0, 163.9, 175.8; HRMS (FAB) m/z : $[\text{M}+\text{H}]^+$ calcd for $\text{C}_{28}\text{H}_{23}\text{O}_7\text{S}$ 503.1164, found 503.1152.

4.26. General procedure for hydrolysis of 3-benzoates

To a solution of a 3-benzoate in EtOH (1.0 mL), 5% NaOH aq. (0.12 mL) was added at 0 °C. The mixture was heated at 60 °C for 15 min. After cooling to rt, the reaction was quenched with water and acidified with 2 N HCl. After extraction with EtOAc and 5% MeOH/EtOAc, the combined organic layers were washed with brine, dried over Na_2SO_4 , and concentrated *in vacuo*. The residue was purified using chromatography on silica gel eluting with EtOAc–hexanes to yield the related 3-hydroxy flavones.

4.26.1. 2-(Benzo[b]thiophen-3-yl)-3-hydroxy-5,7-diisopropoxy-6-methoxy-4H-chromen-4-one (16)

90% yield. ^1H NMR (400 MHz, CDCl_3) δ 1.42 [6H, d, $J = 6.0$ Hz, $\text{OCH}(\text{CH}_3)_2$], 1.49 [6H, d, $J = 6.4$ Hz, $\text{OCH}(\text{CH}_3)_2$], 3.89 (3H, s, OMe), 4.65–4.79 [2H, m, $\text{OCH}(\text{CH}_3)_2$], 6.79 (1H, s, H-8), 7.28 (1H, s, 3-OH), 7.41–7.55 (2H, m, 5'-H and 6'-H), 7.94 (1H, d, $J = 8.0$ Hz, H-4'), 8.40 (1H, d, $J = 8.0$ Hz, H-7'), 8.44 (1H, s, H-2'); ^{13}C NMR (150 MHz, CDCl_3) δ 21.9, 22.4, 60.9, 71.6, 77.8, 97.2, 110.6, 122.9, 124.3, 124.86, 124.88, 126.0, 131.0, 136.6, 137.8, 140.0, 141.1, 141.4, 150.0, 153.7, 156.7, 171.4; HRMS (FAB) m/z : $[\text{M}+\text{H}]^+$ calcd for $\text{C}_{24}\text{H}_{25}\text{O}_6\text{S}$ 441.1372, found 441.1378.

4.26.2. 2-(Benzo[b]thiophen-3-yl)-3,5-dihydroxy-7-isopropoxy-6-methoxy-4H-chromen-4-one (19)

65% yield. ^1H NMR (400 MHz, CDCl_3) δ 1.48 [6H, d, $J = 6.0$ Hz, $\text{OCH}(\text{CH}_3)_2$], 3.92 (3H, s, OMe), 4.79–4.71 [1H, m, $\text{OCH}(\text{CH}_3)_2$], 6.58 (1H, s, 8-H), 6.60 (1H, s, 3-OH, disappears in D_2O), 7.56–7.43 (2H, m, 5'-H and 6'-H), 7.96 (1H, d, $J = 8.0$ Hz, 4'-H), 8.40 (1H, d, $J = 8.0$ Hz, 7'-H), 8.50 (1H, s, 2'-H), 11.67 (1H, s, 5-OH, disappears in D_2O); ^{13}C NMR (150 MHz, CDCl_3) δ 22.0, 60.8, 71.8, 92.4, 104.4, 122.9, 124.3, 125.06, 125.12, 125.6, 132.2, 133.3, 136.1, 136.4, 139.9, 144.2, 152.0, 152.2, 158.0, 174.9; HRMS (FAB) m/z : $[\text{M}+\text{H}]^+$ calcd for $\text{C}_{21}\text{H}_{19}\text{O}_6\text{S}$ 399.0902, found 399.0889.

4.26.3. 2-(Benzo[b]thiophen-3-yl)-3-hydroxy-5,6,7-trimethoxy-4H-chromen-4-one (23)

53% yield. ^1H NMR (400 MHz, CDCl_3) δ 3.95 (3H, s, OCH_3), 4.03 (3H, s, OCH_3), 4.06 (3H, s, OCH_3), 6.83 (1H, s, 8-H), 7.54–7.44 (2H, m, 5'-H and 6'-H), 7.95 (1H, d, $J = 8.0$ Hz, 4'-H), 8.43 (1H, d, $J = 8.0$ Hz, 7'-H), 8.47 (1H, s, 2'-H); ^{13}C NMR (150 MHz, CDCl_3) δ 56.6, 61.7, 62.4, 96.0, 110.2, 123.0, 124.3, 125.0, 125.9, 131.3, 136.6, 138.0, 140.0, 140.3, 141.7, 152.0, 153.6, 158.4, 171.4; HRMS (FAB) m/z : $[\text{M}+\text{H}]^+$ calcd for $\text{C}_{20}\text{H}_{17}\text{O}_6\text{S}$ 385.0746, found 385.0731.

4.26.4. 2-(Benzo[b]thiophen-3-yl)-3-hydroxy-6,7-methylenedioxy-4H-chromen-4-one (25)

65% yield. NMR (400 MHz, CDCl_3) δ 6.14 (2H, s, $-\text{OCH}_2\text{O}-$), 6.97 (1H, brs, 3-OH), 7.06 (1H, s, 8-H), 7.52–7.43 (2H, m, 5'-H and 6'-H), 7.56 (1H, s, 5-H), 7.94 (1H, d, $J = 7.2$ Hz, 4'-H), 8.44 (d, 1H, $J = 8.4$ Hz, 7'-H), 8.50 (1H, s, 2'-H); ^{13}C NMR (150 MHz, CDCl_3) δ 97.9, 101.6, 102.6, 115.9, 122.9, 124.3, 125.0, 125.8, 131.5, 136.5, 137.8, 139.9, 143.3, 146.1, 152.7, 153.2, 171.7; HRMS (FAB) m/z : $[\text{M}+\text{H}]^+$ calcd for $\text{C}_{18}\text{H}_{11}\text{O}_5\text{S}$ 339.0327, found 339.0334.

4.26.5. 2-(Benzo[*b*]thiophen-3-yl)-6,7-dimethoxy-3-hydroxy-4*H*-chromen-4-one (27)

57% yield. ^1H NMR (400 MHz, CDCl_3) δ 4.03 (3H, s, OCH_3), 4.07 (3H, s, OCH_3), 6.96 (1H, brs, 3-OH), 7.03 (1H, s, 8-H), 7.55-7.44 (2H, m, 5'-H and 6'-H), 7.58 (1H, s, 5-H), 7.96 (1H, d, $J = 8.0$ Hz, 4'-H), 8.47 (1H, d, $J = 7.6$ Hz, 7'-H), 8.50 (1H, s, 2'-H); ^{13}C NMR (150 MHz, CDCl_3) δ 56.4, 56.6, 99.5, 103.7, 114.4, 122.9, 124.3, 124.9, 125.0, 126.0, 131.4, 136.6, 137.9, 139.9, 143.2, 147.7, 151.5, 154.9, 171.8; HRMS (FAB) m/z : $[\text{M}+\text{H}]^+$ calcd for $\text{C}_{19}\text{H}_{15}\text{O}_5\text{S}$ 355.0640, found 355.0643.

4.27. General procedure for methylation of 3-hydroxy flavones

To a solution of the related 3-hydroxy flavone in acetone (2.0 mL), K_2CO_3 (2.0 mol eq.) and dimethyl sulfide (1.5 mol eq.) were added at 0 °C. The mixture was refluxed for 4 h. After cooling to rt, the reaction was quenched with water and acidified with 2 N HCl. The mixture was extracted with EtOAc and 5% MeOH/EtOAc, and the combined organic layers were washed with brine, dried over Na_2SO_4 , and concentrated *in vacuo*. The residue was purified using chromatography on silica gel eluting with EtOAc–hexanes to yield the related 3-methoxy flavones.

4.27.1. 2-(Benzo[*b*]thiophen-3-yl)-5,7-diisopropoxy-3,6-dimethoxy-4*H*-chromen-4-one (17)

91% yield. ^1H NMR (400 MHz, CDCl_3) δ 1.41 [6H, d, $J = 6.4$ Hz, $\text{OCH}(\text{CH}_3)_2$], 1.46 [6H, d, $J = 6.4$ Hz, $\text{OCH}(\text{CH}_3)_2$], 3.79 (3H, s, OMe), 3.88 (3H, s, OMe), 4.73–4.60 [2H, m, $\text{OCH}(\text{CH}_3)_2$], 6.72 (1H, s, 8-H), 7.53–7.42 (2H, m, 5'-H and 6'-H), 7.95 (1H, d, $J = 6.0$ Hz), 8.23 (1H, d, $J = 7.2$ Hz, 7'-H), 8.30 (1H, s, 2'-H); ^{13}C NMR (150 MHz, CDCl_3) δ 21.9, 22.4, 60.4, 60.9, 71.5, 78.0, 97.3, 113.7, 122.8, 124.1, 124.9, 125.0, 125.7, 131.5, 136.9, 139.8, 141.3, 141.6,

150.7, 151.1, 153.6, 156.1, 173.5; HRMS (FAB) m/z : $[M+H]^+$ calcd for $C_{25}H_{27}O_6S$ 455.1528, found 455.1520.

4.27.2. *2-(Benzo[b]thiophen-3-yl)-3-hydroxy-7-isopropoxy-5,6-dimethoxy-4H-chromen-4-one*
(**20**)

15 (10.9 mg, 0.022 mmol) was methylated and hydrolyzed by the above procedure to produce **20** (6.6 mg, 2 steps, 74%). 1H NMR (400 MHz, $CDCl_3$) δ 1.49 [6H, d, $J = 6.1$ Hz, $OCH(CH_3)_2$], 3.91 (3H, s, OCH_3), 4.06 (3H, s, OCH_3), 4.72–4.78 [1H, m, $OCH(CH_3)_2$], 6.80 (1H, s, 8-H), 7.42–7.54 (2H, m, 5'-H and 6'-H), 7.95 (1H, d, $J = 7.9$ Hz, 4'-H), 8.40 (1H, d, $J = 8.6$ Hz, 7'-H), 8.44 (1H, s, 2'-H); ^{13}C NMR (150 MHz, $CDCl_3$) δ 21.9, 61.4, 62.3, 71.7, 97.4, 109.8, 122.9, 124.2, 124.87, 124.90, 125.9, 131.1, 136.6, 137.9, 139.9, 140.8, 141.4, 152.2, 153.6, 156.8, 171.3; HRMS (FAB) m/z : $[M+H]^+$ calcd for $C_{22}H_{21}O_6S$ 413.1059, found 413.1072.

4.27.3. *2-(Benzo[b]thiophen-3-yl)-5-hydroxy-7-isopropoxy-3,6-dimethoxy-4H-chromen-4-one*
(**18**)

The title compound (4.4 mg, 31% based on recovery of starting material) was prepared from **17** (15.5 mg, 0.03 mmol) using the same synthetic procedure as for **7**. 1H NMR (400 MHz, $CDCl_3$) δ 1.46 [6H, d, $J = 5.6$ Hz, $OCH(CH_3)_2$], 3.84 (3H, s, OMe), 3.91 (3H, s, OMe), 4.75–4.67 [1H, m, $OCH(CH_3)_2$], 6.52 (1H, s, 8-H), 7.54–7.44 (2H, m, 5'-H and 6'-H), 7.96 (1H, d, $J = 7.2$ Hz, 4'-H), 8.23 (1H, d, $J = 8.0$ Hz, 7'-H), 8.38 (1H, s, 2'-H), 12.57 (1H, s, OH); ^{13}C NMR (150 MHz, $CDCl_3$) δ 21.9, 60.5, 60.8, 71.7, 92.1, 106.6, 122.9, 124.0, 125.1, 125.2, 125.3, 132.6, 133.4, 136.6, 139.3, 139.7, 152.2, 153.3, 153.7, 157.6, 178.6; HRMS (FAB) m/z : $[M+H]^+$ calcd for $C_{22}H_{21}O_6S$ 413.1059, found 413.1047.

4.27.4. 2-(Benzo[*b*]thiophen-3-yl)-7-isopropoxy-3,5,6-trimethoxy-4*H*-chromen-4-one (**21**)

The title compound (5.1 mg, 87%) was prepared from **20** (5.7 mg, 0.014 mmol) using the same synthetic procedure as for **17**. ¹H NMR (400MHz, CDCl₃) δ 1.46 [6H, d, *J* = 6.1 Hz, OCH(CH₃)₂], 3.84 (3H, s, OCH₃), 3.90 (3H, s, OCH₃), 4.04 (3H, s, OCH₃), 4.69–4.74 [1H, m, OCH(CH₃)₂], 6.74 (1H, s, H-8), 7.42-7.53 (2H, m, H-5' and H-6'), 7.94 (1H, d, *J* = 7.3 Hz, H-4'), 8.21 (1H, d, *J* = 7.3 Hz, H-7'), 8.23 (1H, s, H-2'); ¹³C NMR (150 MHz, CDCl₃) δ 21.8, 60.2, 61.4, 62.2, 71.6, 97.5, 113.1, 122.9, 124.0, 124.9, 125.0, 125.7, 131.6, 136.9, 139.8, 139.8, 141.0, 141.4, 151.2, 152.9, 153.5, 156.3, 173.4; HRMS (FAB) *m/z*: [M+H]⁺ calcd for C₂₃H₂₃O₆S 427.1215, found 427.1220.

4.27.5. 2-(Benzo[*b*]thiophen-3-yl)-3-benzoyloxy-5,6,7-trimethoxy-4*H*-chromen-4-one (**22**)

The title compound was prepared from 6-hydroxy-2,3,4-trimethoxyacetophenone and **42** using the same procedure as that of **14** from **39** and **42**. ¹H NMR (400 MHz, CDCl₃) δ 3.94 (3H, s, OCH₃), 4.00 (3H, s, OCH₃), 4.01 (3H, s, OCH₃), 6.81 (1H, s, 8-H), 7.62-7.42 (5H, m, 5'-H, 6'-H, 3''-H, 4''-H and 5''-H), 7.90 (1H, d, *J* = 7.6 Hz, 4'-H), 8.03 (1H, s, 2'-H), 8.14 (2H, dd, *J* = 1.4 and 8.2 Hz, 2''-H and 6''-H), 8.19 (1H, d, *J* = 8.0 Hz, 7'-H); ¹³C NMR (100 MHz, CDCl₃) δ 56.4, 61.6, 62.3, 96.0, 113.0, 122.8, 123.7, 125.0, 125.2, 128.6, 130.5, 131.1, 133.8, 134.3, 136.6, 139.8, 140.7, 151.5, 152.8, 153.9, 158.2, 164.0, 170.2; HRMS (FAB) *m/z*: [M+H]⁺ calcd for C₂₇H₂₁O₇S, 489.1008, found 489.0994.

4.27.6. 2-(Benzo[*b*]thiophen-3-yl)-3-benzoyloxy-6,7-methylenedioxy-4*H*-chromen-4-one (**24**)

The title compound was prepared from 2-hydroxy-4,5-methylenedioxyacetophenone and **42** using the same procedure as that of **14** from **39** and **42**. ^1H NMR (400 MHz, CDCl_3) δ 6.16 (2H, s, $-\text{OCH}_2\text{O}-$), 7.01 (1H, s, 8-H), 7.63-7.42 (6H, m, 5-H, 5'-H, 6'-H, 3''-H, 4''-H and 5''-H), 7.90 (1H, d, $J = 8.0$ Hz, 4'-H), 8.06 (1H, s, 2'-H), 8.14 (2H, m, 2''-H and 6''-H), 8.19 (1H, d, $J = 7.2$ Hz, 7'-H); ^{13}C NMR (100 MHz, CDCl_3) δ 97.9, 102.6, 102.7, 119.0, 122.8, 123.8, 125.1, 125.2, 128.5, 128.6, 130.5, 131.3, 133.9, 134.0, 136.6, 139.7, 146.5, 152.9, 153.2, 163.9, 170.9; HRMS (FAB) m/z : $[\text{M}+\text{H}]^+$ calcd for $\text{C}_{25}\text{H}_{15}\text{O}_6\text{S}$, 443.0589, found 443.0587.

4.27.7. 2-(Benzo[b]thiophen-3-yl)-3-benzoyloxy-6,7-dimethoxy-4H-chromen-4-one (**26**)

The title compound was prepared from 2-hydroxy-4,5-dimethoxyacetophenone and **42** using the same procedure as that of **14** from **39** and **42**. ^1H NMR (400 MHz, CDCl_3) δ 4.01 (3H, s, OCH_3), 4.04 (3H, s, OCH_3), 7.01 (1H, s, 8-H), 7.63-7.43 (5H, m, 5'-H, 6'-H, 3''-H, 4''-H and 5''-H), 7.64 (1H, s, 5-H), 7.91 (1H, d, $J = 8.0$ Hz, 4'-H), 8.05 (1H, s, 2'-H), 8.14 (2H, dd, $J = 1.0$ and 8.6 Hz, 2''-H and 6''-H), 8.21 (1H, d, $J = 8.0$ Hz, 7'-H); ^{13}C NMR (150 MHz, CDCl_3) δ 56.4, 56.6, 99.5, 104.7, 117.4, 122.8, 123.8, 125.2, 125.3, 128.6, 130.5, 131.2, 133.8, 134.1, 136.6, 139.8, 147.9, 151.7, 152.9, 154.8, 164.0, 171.0; HRMS (FAB) m/z : $[\text{M}+\text{H}]^+$ calcd for $\text{C}_{26}\text{H}_{19}\text{O}_6\text{S}$, 459.0902, found 459.0884.

4.28. Antiproliferative activity assay

Cells were cultured in RPMI-1640 medium supplemented with 25 mM HEPES, 0.25% sodium bicarbonate (Gibco), 10% fetal bovine serum (Millipore-Sigma), and 1 \times Antibiotic-Antimycotic (Gibco) mixture. Freshly trypsinized cell suspensions were seeded in 96-well microtiter plates at densities of 4,000-11,000 cells per well, with diluted compounds with

medium prepared from DMSO stock solutions. The highest concentration of DMSO in the cultures (0.1% v/v) was used without effect on cell growth under the culture conditions. After 72 h in culture, attached cells were fixed in cold 10% trichloroacetic acid and then stained with 0.04% SRB. Absorbance at 515 nm was measured using a microplate reader (ELx800, BioTek) after solubilizing the bound dye. The mean IC_{50} is the concentration of agent that reduced cell growth by 50% compared with vehicle (0.1% DMSO) control under the experimental conditions used and is the average from at least three independent experiments with duplicate samples. The following human tumor cell lines were used in the assay: A549 (lung carcinoma), KB (cervical cancer cell line; HeLa derivative), KB-VIN (vincristine-resistant KB subline showing MDR phenotype by overexpressing P-gp), MCF-7 (estrogen receptor positive, HER2-negative breast cancer), PC-3 (androgen-insensitive prostate cancer). All cell lines were obtained from the Lineberger Comprehensive Cancer Center (UNC-CH) or from ATCC (Manassas, VA), except KB-VIN, which was a generous gift of Professor Y.-C. Cheng (Yale University). MDR stock cells (KB-VIN) were maintained in the presence of 100 nM vincristine.

Antiproliferative activity against HUVECs was assessed by cell viability assay using a WST-8 [2-(2-methoxy-4-nitrophenyl)-3-(4-nitrophenyl)-5-(2,4-disulfophenyl)-2H-tetrazolium] based Cell Count Reagent SF (Nacalai Tesque, Japan). HUVECs (2,500 cells/well) were seeded on a 96-well plate for 24 h and then co-treated for 48 h at 37 °C with 30 ng/mL vascular endothelial growth factor (VEGF) (Sigma-Aldrich) and a series of dilutions of compounds to be tested. Cell viability was calculated by measuring absorbance at 450 nm.

4.29. Cell cycle analysis

Distribution of cells in the cell cycle was evaluated by measurement of cellular DNA content by propidium iodide (PI) staining in the presence of RNase (BD Biosciences). Briefly, cells were seeded in 12-well culture plates 24 h prior to treatment with compounds. After a 24 h treatment, supernatants and trypsinized cells were collected, followed by centrifugation for 5 min at 800 x g. The pellet was resuspended with PBS and fixed in 70% EtOH overnight at -20 °C, followed by staining with PI/RNase for 30 min at 37 °C. Stained cells were analyzed by flow cytometry (LSRFortessa, BD Biosciences). Experiments were repeated a minimum of two times.

4.30. Immunofluorescence staining

Cells were grown on an 8-well chamber slide (Lab-Tech) for 24 h prior to treatment with compound at equitoxic compound concentrations as described previously [19]. The equitoxic compound concentrations used were based on their IC₅₀ values. After treatment of cells with agent for 24 h, cells were fixed with 4% paraformaldehyde in PBS and permeabilized with 0.5% Triton X-100 in PBS. Fixed cells were labeled with mouse monoclonal antibody to α -tubulin (B5-1-2, Sigma) and rabbit IgG to Ser10-phosphorylated histone H3 (p-H3) (#06-570, EMD Millipore) or rabbit polyclonal antibody to γ -H2AX (BETHYL Lab), followed by FITC-conjugated antibody to mouse IgG (Sigma) and Alexa Fluor 549-conjugated antibody to rabbit IgG (Life Technologies). DNA was labeled with DAPI (Sigma). Fluorescently labeled cells were observed using a confocal microscope (Zeiss, LSM700) with ZEN (black edition) software (Zeiss). The images shown in the figures were a projection of 14-24 optical sections. Final images were prepared using Adobe Photoshop CS6.

4.31. Tubulin assays

Inhibitory effects of compounds against electrophoretically homogeneous bovine brain tubulin were as described previously [40, 41]. In the inhibition of colchicine binding to tubulin assays, 0.5 μM tubulin was incubated with 5.0 μM [^3H]colchicine from Perkin-Elmer and 5.0 μM test compound at 37 $^{\circ}\text{C}$ for 10 min. Other reaction components were summarized previously and the method described in great detail [41], based on earlier studies describing the stabilization of the colchicine binding activity to tubulin [42]. In brief, each 0.1 mL reaction also contained 1.0 M monosodium glutamate (taken from a 2.0 M stock solution adjusted to pH 6.6 with HCl), 1.0 mM MgCl_2 , 1.0 mM GTP, 0.5 mg/mL bovine serum albumin and 0.1 M glucose-1-phosphate. The 10 min incubation time was chosen since the reaction was about 40-60% complete at that time point. Reactions were stopped with 2.0 mL of ice-cold water and poured over a single Whatman DEAE-cellulose 2.5 cm filter. The sample was allowed to drip through the filter by gravity, and then the filter was washed three times under vacuum, each time with 2.0 mL of ice-cold water. Each filter was placed into 5 mL of scintillation cocktail and counted 18 h later in a Beckman liquid scintillation counter. Compound containing samples were compared to samples containing no inhibitor, and all sample values were corrected for background reaction mixtures containing no tubulin.

The assay for measurement of inhibition of tubulin assembly was described in detail before [40]. To summarize the method, reaction mixtures contained 1.0 mg/mL (10 μM) tubulin, 0.8 M monosodium glutamate, 4% (v/v) dimethyl sulfoxide and varying compound concentrations and were preincubated for 15 min at 30 $^{\circ}\text{C}$ without guanosine 5'-triphosphate (GTP) in a 0.24 mL reaction volume. The samples were placed on ice, and 0.4 mM repurified (> 99% purity) GTP was added (10 μL of a 10 mM solution). Compound concentrations were based on the final 0.25

mL reaction volume. Reaction mixtures were transferred to 0 °C cuvettes in Beckman DU7400/7500 recording spectrophotometers equipped with Peltier temperature controllers specified by the manufacturer to maintain temperature within the cuvettes in the range from 0 to 100 °C (confirmed in our laboratory with a temperature probe for the range from 0 to 37 °C). Turbidity development was measured at 350 nm, and the reactions were followed at 30 °C for 20 min following a rapid (< 30 s) temperature jump to 30 °C. Microtubule assembly was always confirmed by a reverse temperature jump to 0 °C, taking about 2 min. “Normal” microtubules are cold-labile, and this step distinguishes “normal” polymer from polymer induced by such drugs as paclitaxel, which are generally cold-stable [43], and from a variety of structurally aberrant polymers that display varying cold lability, but that are generally more cold stable than the normal polymer [44, 45]. IC₅₀ values were obtained first in range finding studies and then with two to three detailed experiments with compounds (concentrations refer to the final 0.25 mL reaction volumes) within a narrow range of values selected from 0.4, 0.5, 0.75, 1.0, 1.5, 2.0, 3.0, 4.0, 5.0, 7.5, 10, 15 and 20 μM. Compound concentrations as IC₅₀ values that inhibited increase in turbidity by 50% relative to a control sample were determined by interpolation between a concentration inhibiting turbidity development < 50% and the next highest concentration inhibiting turbidity development > 50%, using semi-logarithmic graph paper. Note that the Beckman cuvette holders hold six samples, one of which is always a control, so that a maximum of 5 compound concentrations can be examined in one experiment. The Beckman spectrophotometers are computer driven, and the program used to evaluate polymerization inhibition was written by Mr. M. D. Boland, formerly a Beckman technician, doing business as MDB Analytical Associates, South Plainfield, NJ.

4.32. *Topo I assay*

The assay was performed as described in the literature [46]. A 15 μ L reaction mixture containing 35 mM Tris-HCl (pH 8.0), 72 mM KCl, 5 mM MgCl₂, 5 mM dithiothreitol, 5 mM spermidine, 0.01% bovine serum albumin, 1 U Topo I (Takara Bio), and a series of compound concentrations was preincubated for 5 min at 37 °C. After a 30 min incubation at 37 °C with 250 ng supercoiled pBR322 plasmid DNA (Takara Bio), DNA was separated by 0.8% agarose gel electrophoresis and stained with ethidium bromide for 30 min. Flavonol **20** was used at 250, 500, 750 and 1000 μ M. CPT was used at 250 and 500 μ M. All reaction mixtures contained 6.6% DMSO, which was also used as a negative control.

4.33. *Computer modeling*

Three-dimensional (3D) structures of tubulin-ligand complexes were predicted by GOLD 5.1 software [47] with default settings. The 3D structures of tubulin (TUBA1A and TUBB2B) and DNA Topo I used in this study were constructed from the Protein Data Bank (PDB) entries (PDB IDs: 1SA0 and 1T8I, respectively).

For the tubulin docking model, missing hydrogen atoms in the crystal structure were computationally added by Hermes [48]. The center of the active site was defined as the center of the ligand in 1SA0, and the active site radius was set to 10.0 Å. For the docking calculations, the quantum-chemically optimized structures of ligands were used as initial structures. The structural optimizations of ligands were carried out by B3LYP/6-311+G(df,p) using Gaussian 09, Revision B.01 [49].

For the Topo I docking model, the entry 1T8I includes a DNA Topo I, a 22-base-pair DNA (22bp DNA), and CPT. To obtain the 3D structure of the complex with compound **20**, CPT

was deleted from the entry 1T8I. The geometry of compound **20** was optimized by density functional theory calculations at the B3LYP/6-311G(d) level of theory using Gaussian 16 software [49]. Compound **20** was docked in the ligand-binding pocket to which CPT was originally bound in the complex with DNA topoisomerase I and a 22bp DNA. For computational docking, the GOLD program [50] was used.

4.34. *In vitro* metabolic study

The NADPH-dependent microsomal metabolic reaction was performed in 86 mM potassium phosphate buffer (pH 7.4) containing 5 mM MgCl₂, 5 mM NADPH, and 80 μM compound, with 0.4% DMSO as a control. After preincubation of reaction mixtures at 37 °C, 0.5 mg of human liver microsomes (UltraPool Human Liver S9, 150-Donor Pool, Mixed Gender from Corning, #452116) was added and incubated at 37 °C. Reactions were terminated after 60, 120, or 180 min by adding 1.5 volume of ice-cold acetonitrile, followed by centrifugation for 5 min at 15,000 x g at 0 °C. The supernatant was analyzed by HPLC using an InertSustain C18 (5 μm, 4.6 mm × 150 mm, GL Science) column with 80% MeCN in H₂O at a flow rate of 0.5 mL/min. The column eluant was monitored at 254 nm. The peak heights were converted to percentage drug remaining, using the initial time (0 min) peak height values as 100%. For determination of NADPH-dependent microsomal metabolic half-life ($t_{1/2}$), the slope of the linear regression from log percentage remaining versus incubation time relationships ($-k$) was used in the conversion to an *in vitro* $t_{1/2}$ by the formula: *in vitro* $t_{1/2} = 0.693/k$. Conversion to *in vitro* CL_{int} (in units of mL/min/mg protein) was performed using the formula: CL_{int} = (0.693/*in vitro* $t_{1/2}$) × (mL incubation / mg microsomes).

Author Contributions

Y.S., M.G., and K.N.G. designed this study. Y.S., Y.T., S.H., H.T., and K.N.G. designed and performed chemical experiments. Y.M., E.H., K.Y., and M.G. designed and performed biological experiments. T.N. and A.O. performed computer modeling. Y.S., M.G. and K.N.G. evaluated all results and wrote the manuscript. All authors have given approval to the final version of the manuscript.

Notes

The authors declare no competing financial interest.

Acknowledgements

We wish to thank the Microscopy Service Laboratory (UNC-CH) for their expertise in confocal microscopy. In addition, we appreciate critical comments, suggestions, and editing of the manuscript by Dr. Susan L. Morris-Natschke (UNC-CH). We also thank Dr. Toshiyuki Atsumi (Kyushu University of Health and Welfare, Japan) for assay of antiproliferative activity against HUVECs. This study was supported by a Grant-in-Aid from the Ministry of Education, Culture, Sports, Science and Technology (MEXT KAKENHI, Japan) awarded to K.N.G. (Grant Number 25293024, 18H02583), Y. S. (Grant Number 18K14344), A.O. (Grant Number 17K08257), and T.N. (Grant Number 19J23595), as well as by a grant from the IBM Junior Faculty Development Awards awarded to M.G.

Disclaimer

This research was supported in part by the Developmental Therapeutics Program in the Division of Cancer Treatment and Diagnosis of the National Cancer Institute, which includes federal funds under Contract No. HHSN261200800001E. The content of this publication does not

necessarily reflect the views or policies of the Department of Health and Human Services, nor does mention of trade names, commercial products, or organizations imply endorsement by the U.S. Government.

Appendix A. Supplementary data.

Supplementary data related to this article can be found at supporting information, an uploaded file with the manuscript.

References

- [1] K. Sak, Cytotoxicity of dietary flavonoids on different human cancer types. *Pharmacognosy Rev.*, 8 (2014) 122–146.
- [2] J. A. Beutler, J. H. Cardellina II, C. M. Lin, E. Hamel, G. M. Cragg, M. R. Boyd, Centaureidin, a cytotoxic flavone from *Polymnia fruticosa*, inhibits tubulin polymerization. *Bioorg. Med. Chem. Lett.* 3 (1993) 581–584.
- [3] J. J. Lichius, O. Thoison, A. Montagnac, M. País, F. Guéritte-Voegelein, T. Sévenet, J. P. Cosson, A. H. Hadi, Antimitotic and cytotoxic flavonols from *Zieridium pseudobtusifolium* and *Acronychia porteri*. *J. Nat. Prod.* 57 (1994) 1012–1016.
- [4] J. A. Beutler, E. Hamel, A. J. Vlietinck, A. Haemers, P. Rajan, J. N. Roitman, J. H. II, M. R. Boyd, Structure-activity requirements for flavone cytotoxicity and binding to tubulin. *J. Med. Chem.* 41 (1998) 2333–2338.
- [5] L. M. Salonen, M. Ellermann, F. Diederich, Aromatic rings in chemical and biological recognition: energetics and structures. *Angew. Chem. Int. Ed. Engl.* 50 (2011) 4808–4842.
- [6] E. A. Meyer, R. K. Castellano, F. Diederich, Interactions with aromatic rings in chemical and biological recognition. *Angew. Chem. Int. Ed. Engl.* 42 (2003) 1210–1250.

- [7] T. J. Ritchie, S. J. Macdonald, Physicochemical descriptors of aromatic character and their use in drug discovery. *J. Med. Chem.* 57 (2014) 7206–215.
- [8] M. Levitt, M. F. Perutz, Aromatic rings act as hydrogen bond acceptors. *J. Mol. Biol.* 201 (1988) 751–754.
- [9] T. J. Ritchie, S. J. F. Macdonald, R. J. Young, S. D. Pickett, The impact of aromatic ring count on compound developability: further insights by examining carbo- and hetero-aromatic and -aliphatic ring types. *Drug Discovery Today* 16 (2011) 164– 171.
- [10] R. J. Young, D. V. S. Green, C. N. Luscombe, A. P. Hill, A. P. Getting physical in drug discovery II: the impact of chromatographic hydrophobicity measurements and aromaticity. *Drug Discovery Today* 16 (2011) 822– 830.
- [11] Y. Yang, O. Engkvist, A. Llinas, H. Chen, Beyond size, ionization state, and lipophilicity: influence of molecular topology on absorption, distribution, metabolism, excretion, and toxicity for druglike compounds. *J. Med. Chem.* 55 (2012) 3667– 3677.
- [12] T. J. Ritchie, S. J. F. Macdonald, S. Peace, S. D. Pickett, C. N. Luscombe, Increasing small molecule drug developability in sub-optimal chemical space. *Med. Chem. Commun.* 4 (2013) 673– 680.
- [13] R. S. Keri, K. Chand, S. Budagumpi, S. B. Somappa, S. A. Patil, B. M. Nagaraja, An overview of benzo[*b*]thiophene-based medicinal chemistry. *J. Med. Chem.* 138 (2017) 1002– 1033.
- [14] R. D. Taylor, M. MacCoss, A. D. Lawson, Rings in drugs. *J. Med. Chem.* 57 (2014) 5845– 5859.

- [15] K. Nakagawa-Goto, K. F. Bastow, T. H. Chen, S. L. Morris-Natschke, K. H. Lee, Antitumor agents 260. New desmosdumotin B analogues with improved in vitro anticancer activity. *J. Med. Chem.* 51 (2008) 3297–3303.
- [16] K. Nakagawa-Goto, P. C. Chang, C. Y. Lai, H. Y. Hung, T. H. Chen, P. C. Wu, H. Zhu, A. Sedykh, K. F. Bastow, K. H. Lee, Antitumor agents 280. Multidrug resistance-selective desmosdumotin B analogues. *J. Med. Chem.* 53 (2010) 6699–6705.
- [17] K. Nakagawa-Goto, P. C. Wu, C. Y. Lai, E. Hamel, H. Zhu, L. Zhang, T. Kozaka, E. Ohkoshi, M. Goto, K. F. Bastow, K. H. Lee, Antitumor agents 284. New desmosdumotin B analogues with bicyclic B-ring as cytotoxic and antitubulin agents. *J. Med. Chem.* 54 (2011) 1244–1255.
- [18] M. D. Hall, M. D. Handley, M. M. Gottesman, Is resistance useless? Multidrug resistance and collateral sensitivity. *Trends Pharmacol. Sci.* 30 (2009) 546–556.
- [19] K. Nakagawa-Goto, A. Oda, E. Hamel, E. Ohkoshi, K.H. Lee, M. Goto, Development of a novel class of tubulin inhibitor from desmosdumotin B with a hydroxylated bicyclic B-ring. *J. Med. Chem.* 58 (2015) 2378–2389.
- [20] D. Simoni, R. Romagnoli, R. Baruchello, R. Rondanin, M. Rizzi, M. G. Pavani, D. Alloatti, G. Giannini, M. Marcellini, T. Riccioni, M. Castorina, M. B. Guglielmi, F. Bucci, P. Carminati, C. Pisano, Novel combretastatin analogues endowed with antitumor activity. *J. Med. Chem.* 49 (2006) 3143–3152.
- [21] R. Romagnoli, P. G. Baraldi, M. D. Carrion, C. C. Lopez, D. Preti, F. Fruttarolo, M. G. Pavani, M. A. Tabrizi, M. Tolomeo, S. Grimaudo, A. Di Cristina, J. Balzarini, J. A. Hadfield, A. Brancale, E. Hamel, Synthesis and biological evaluation of 2- and 3-

- aminobenzo[*b*]thiophene derivatives as antimitotic agents and inhibitors of tubulin polymerization. *J. Med. Chem.* 50 (2007) 2273–2277.
- [22] Y. H. Chang, M. H. Hsu, S. H. Wang, L. J. Huang, K. Qian, S. L. Morris-Natschke, E. Hamel, S. C. Kuo, K. H. Lee, Design and synthesis of 2-(3-benzo[*b*]thienyl)-6,7-methylenedioxyquinolin-4-one analogues as potent antitumor agents that inhibit tubulin assembly. *J. Med. Chem.* 52 (2009) 4883–4891.
- [23] K. Ester, M. Hranjec, I. Piantanida, I. Caleta, I. Jarak, K. Pavelić, M. Kralj, G. Karminski-Zamola, Novel derivatives of pyridylbenzo[*b*]thiophene-2-carboxamides and benzo[*b*]thieno[2,3-*c*]naphthyridin-2-ones: minor structural variations provoke major differences of antitumor action mechanisms. *J. Med. Chem.* 52 (2009) 2482–2492.
- [24] B. L. Flynn, G. S. Gill, D. W. Grobelny, J. H. Chaplin, D. Paul, A. F. Leske, T. C. Lavranos, D. K. Chalmers, S. A. Charman, E. Kostewicz, D. M. Shackelford, J. Morizzi, E. Hamel, M. K. Jung, G. Kremmidiotis, Discovery of 7-hydroxy-6-methoxy-2-methyl-3-(3,4,5-trimethoxybenzoyl)benzo[*b*]furan (BNC105), a tubulin polymerization inhibitor with potent antiproliferative and tumor vascular disrupting properties. *J. Med. Chem.* 54 (2011) 6014–6027.
- [25] N. R. Penthala, V. N. Sonar, J. Horn, M. Leggas, J. S. Yadlapalli, P. A. Crooks, Synthesis and evaluation of a series of benzothiophene acrylonitrile analogs as anticancer agents. *Med. Chem. Comm.* 4 (2013) 1073–1078.
- [26] A. Lauria, A. Alfio, R. Bonsignore, C. Gentile, A. Martorana, G. Gennaro, G. Barone, A. Terenzi, A. M. Almerico, New benzothieno[3,2-*d*]-1,2,3-triazines with antiproliferative activity: synthesis, spectroscopic studies, and biological activity. *Bioorg. Med. Chem. Lett.* 24 (2014) 3291–3297.

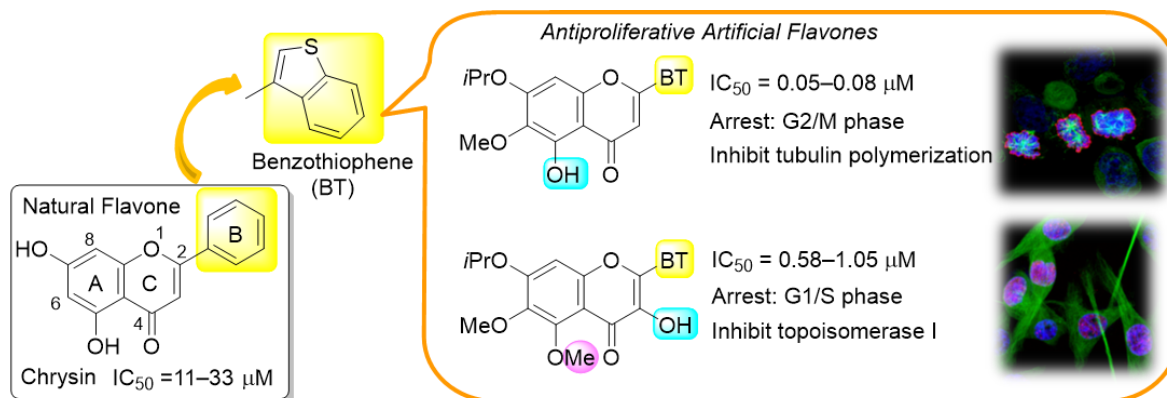
- [27] A. Martorana, C. Gentile, U. Perricone, A. P. Piccionello, R. Bartolotta, A. Terenzi, A. Pace, F. Mingoia, A. M. Almerico, A. Lauria, Synthesis, antiproliferative activity, and *in silico* insights of new 3-benzoylamino-benzo[*b*]thiophene derivatives. *Eur. J. Med. Chem.* 90 (2015) 537–546.
- [28] M. Inuma, K. Iwashima, S. Matsuura, Synthetic studies on flavone derivatives. XIV. Synthesis of 2', 4', 5'-trioxygenated flavones. *Chem. Pharm. Bull.* 32 (1984) 4935–4941.
- [29] P. V. Podea, M. I. Toşa, C. Paizs, F. D. Irimie, Chemoenzymatic preparation of enantiopure *L*-benzofuranyl- and *L*-benzo[*b*]thiophenyl alanines. *Tetrahedron Asym.* 19 (2008) 500–511.
- [30] A. Fougerousse, E. Gonzalez, R. Brouillard, A convenient method for synthesizing 2-aryl-3-hydroxy-4-oxo-4*H*-1-benzopyrans or flavonols. *J. Org. Chem.* 65 (2000) 583–586.
- [31] P. R. Kumar, C. Balakrishna, R. Gudipati, P. K. Hota, A. B. Chaudhary, A. J. Shree, S. Yennam, M. Behera, An efficient synthesis of 8-substituted odoratine derivatives by the Suzuki coupling reaction. *J. Chem. Sci.* 128 (2016) 441–450.
- [32] D. T. Witiak, S. K. Kim, A. K. Tehim, K. D. Sternitzke, R. L. McCreery, S. U. Kim, D. R. Feller, K. J. Romstedt, V. S. Kamanna, H. A. Newman, *J. Med. Chem.* 31 (1988) 1437–1445.
- [33] A. Mendieta, F. Jiménez, L. Garduño-Siciliano, A. Mojica-Villegas, B. Rosales-Acosta, L. Villa-Tanaca, G. Chamorro-Cevallos, J. L. Medina-Franco, N. Meurice, R. U. Gutiérrez, L. E. Montiel, M. C. Cruz, J. Tamariz, Synthesis and highly potent hypolipidemic activity of alpha-asarone- and fibrate-based 2-acyl and 2-alkyl phenols as HMG-CoA reductase inhibitors. *Bioorg. Med. Chem.* 22 (2014) 5871–5882.
- [34] N. Fang, M. Leidig, T. J. Mabry, Fifty-one flavonoids from *Gutierrezia microcephala*. *Phytochemistry* 25 (1986) 927–934.

- [35] Q. Shi, L. Li, J. J. Chang, C. Autry, M. Kozuka, T. Konoshima, J. R. Estes, C. M. Lin, E. Hamel, A. T. McPhail, D. R. McPhail, K. H. Lee, Antitumor agents 154. Cytotoxic and antimetabolic flavonols from *Polanisia dodecandra*. *J. Nat. Prod.* 58 (1995) 475–482.
- [36] G. Lewin, G. Aubert, S. Thoret, J. Dubois, T. Cresteil, Influence of the skeleton on the cytotoxicity of flavonoids. *Bioorg. Med. Chem.* 20 (2012) 1231–1239.
- [37] D. B. Longley, D. P. Harkin, P. G. Johnston, 5-fluorouracil: mechanisms of action and clinical strategies. *Nat. Rev. Cancer* 3 (2003) 330–338.
- [38] I. Y. Torshin, I. T. Weber, R. W. Harrison, Geometric criteria of hydrogen bonds in proteins and identification of ‘bifurcated’ hydrogen bonds. *Protein Eng.* 15 (2002) 359–363.
- [39] McDonald, I.K.; Thornton, J.M. Satisfying hydrogen bonding potential in proteins. *J. Mol. Biol.* **1994**, 238, 777–793.
- [40] E. Hamel, Evaluation of antimetabolic agents by quantitative comparisons of their effects on the polymerization of purified tubulin. *Cell Biochem. Biophys.* 38 (2003) 1–22.
- [41] P. Verdier-Pinard, J. Y. Lai, H. D. Yoo, J. Yu, B. Márquez, D. G. Nagle, M. Nambu, J. D. White, J. R. Falck, W. H. Gerwick, B. W. Day, E. Hamel, Structure-activity analysis of the interaction of curacin A, the potent colchicine site antimetabolic agent, with tubulin and effects of analogs on the growth of MCF-7 breast cancer cells. *Mol. Pharmacol.* 53 (1998) 62–76.
- [42] E. Hamel, C. M. Lin, Stabilization of the colchicine-binding activity of tubulin by organic acids. *Biochim. Biophys. Acta* 675 (1981) 226–231.
- [43] S. Grover, J. M. Rimoldi, A. A. Molinero, A. G. Chaudhary, D. G. I. Kingston, E. Hamel, Differential effects of paclitaxel (Taxol) analogs modified at positions C-2, C-7, and C-3' on tubulin polymerization and identification of a hyperactive paclitaxel derivative. *Biochemistry* 34 (1995) 3927–3934.

- [44] R. Bai, E. Hamel, (-)-Rhazinilam and the diphenylpyridazinone NSC 613241: two compounds inducing the formation of morphologically similar tubulin spirals but binding apparently to two distinct sites on tubulin. *Arch. Biochem. Biophys.* 604 (2016) 63-73.
- [45] R. Bai, Z. Cruz-Monserrate, W. Fenical, G.R. Pettit, E. Hamel, Interaction of diazonamide A with tubulin. *Arch. Biochem. Biophys.* 680 (2020) 108217.
- [46] J. L. Nitiss, E. Soans, A. Rogojina, A. Seth, M. Mishina, Topoisomerase assays. *Curr. Protoc. Pharmacol.* (2012) Chapter 3.
- [47] G. Jones, P. Willett, R. C. Glen, Molecular recognition of receptor sites using a genetic algorithm with a description of desolvation. *J. Mol. Biol.* 245 (1995) 43-53.
- [48] Hermes 5.1, CCDC Software Ltd.: Cambridge, UK, 2012.
- [49] M. J. Frisch, G. W. Trucks, H. B. Schlegel, G. E. Scuseria, M. A. Robb, J. R. Cheeseman, G. Scalmani, V. Barone, B. Mennucci, G. A. Petersson, H. Nakatsuji, M. Caricato, X. Li, H. P. Hratchian, A. F. Izmaylov, J. Bloino, G. Zheng, J. L. Sonnenberg, M. Hada, M. Ehara, K. Toyota, R. Fukuda, J. Hasegawa, M. Ishida, T. Nakajima, Y. Honda, O. Kitao, H. Nakai, T. Vreven, J. A. Montgomery, J. E. Peralta, Jr., F. Ogliaro, M. Bearpark, J. J. Heyd, E. Brothers, K. N. Kudin, V. N. Staroverov, T. Keith, R. Kobayashi, J. Normand, K. Raghavachari, A. Rendell, J. C. Burant, S. S. Iyengar, J. Tomasi, M. Cossi, N. Rega, J. M. Millam, M. Klene, J. E. Knox, J. B. Cross, V. Bakken, C. Adamo, J. Jaramillo, R. Gomperts, R. E. Stratmann, O. Yazyev, A. J. Austin, R. Cammi, C. Pomelli, J. W. Ochterski, R. L. Martin, K. Morokuma, V. G. Zakrzewski, G. A. Voth, P. Salvador, J. J. Dannenberg, S. Dapprich, A. D. Daniels, O. Farkas, J. B. Foresman, J. V. Ortiz, J. Cioslowski, D. J. Fox, *Gaussian 09 (Revision B.01)*, Gaussian, Inc.: Wallingford, CT, 2010; *Gaussian 16, Revision A.03*, Gaussian, Inc., Wallingford CT, 2016.

- [50] G. Jones, P. Willett, R. C. Glen, A. R. Leach, R. Taylor, Development and validation of a genetic algorithm for flexible docking. *J. Mol. Biol.* 267 (1997) 727–748.

Graphical Abstract



Journal Pre-proof

Highlights (85 characters with space, each)

- ▶ Benzo[*b*]thiophenyl(BT) chromone was discovered as a new antitumor scaffold.
- ▶ Small changes of functional groups induced distinct biological profiles.
- ▶ 5-OH BT-chromone derivatives arrested cell cycle progression at the G2/M phase by inhibition of tubulin assembly.
- ▶ 3-OH BT-chromone derivatives affected the G1/S phase by inducing DNA damage through inhibition of Topo I.
- ▶ The binding mode to the target protein was discussed by a docking model.

Journal Pre-proof

Declaration of Interest Statement

Manuscript entitled “Effects of substituent pattern on the intracellular target of antiproliferative benzo[*b*]thiophenyl chromone derivatives” by Yohei Saito, Yukako Taniguchi, Sachika Hirazawa, Yuta Miura, Hiroyuki Tsurimoto, Tomoki Nakayoshi, Akifumi Oda, Ernest Hamel, Katsumi Yamashita, Masuo Goto, and Kyoko Nakagawa-Goto.

The authors declare no conflicts of interest associated with this manuscript.

Feb. 10, 2021

Kyoko Nakagawa-Goto, Ph.D.